Geochemistry

The geochemistry of leucite-bearing lavas from early stages of the Somma-Vesuvius volcanic complex: feeder systems and mantle enrichment processes in the Neapolitan district of the Roman Magmatic Province

--Manuscript Draft--

Manuscript Number:	
Article Type:	Research Paper
Keywords:	leucite tephrites; leucite-bearing shoshonites; leucite-free shoshonites; ultrapotassic volcanism; Somma-Vesuvius; Neapolitan district; Roman Province
Corresponding Author:	Vincenza Guarino Universita degli Studi di Napoli Federico II Dipartimento di Scienze della Terra dell'Ambiente e delle Risorse ITALY
First Author:	Vincenza Guarino
Order of Authors:	Vincenza Guarino
	Roberto Solone
	Martina Casalini
	Luigi Franciosi
	Luigi Dallai
	Vincenzo Morra
	Sandro Conticelli
	Leone Melluso
Abstract:	The lavas of the Monte Somma activity (early stage of the Somma-Vesuvius volcanic complex) are mildly differentiated plagioclase-clinopyroxene-olivine- ± leucite-bearing lavas (leucite tephrites, leucite-bearing shoshonites, latites), low in MgO, Cr and Ni, with a Sr-Nd-isotope range (87Sr/86Sr = 0.706865-0.707861; 143Nd/144Nd = 0.51244-0.51258) overlapping that of the Vesuvian lavas late after 1638 CE (late stage of the Somma-Vesuvius volcanic complex). The differentiation is dominated by fractional crystallization of clinopyroxene, calcic plagioclase, olivine and leucite, with limited interaction with crustal rocks. Oxygen isotopes on clinopyroxene and olivine phenocrysts (δ18O = 6.5-7.9 ‰) are higher than typical uncontaminated mantle magmas. However, these values are also not fully consistent with the sole open-system assimilation+fractional crystallization of a mantle-derived ultrapotassic magma. A contribution from a recycled crustal component in the mantle source is required, likely dominated by sediment-derived fluids and melts. The Somma lavas are characterized by distinctly different geochemical features compared to the mafic products of the neighboring volcanic areas (i.e., Phlegrean Fields, Procida and Ischia volcanoes), where the recycled crustal component is less pronounced.
Suggested Reviewers:	Dejan Prelević dejan.prelevic@rgf.bg.ac.rs He is an expert on Somma-Vesuvius magmatism
	Rajesh Srivastava rajeshgeolbhu@gmail.com He is an expert on undersaturated alkaline magmatism
	Vladica Cvetkovic vladica.cvetkovic@rgf.bg.ac.rs He is an expert in the field of orogenic magmatism in the Mediterranean region
	Gianluca Bianchini gianluca.bianchini@unife.it He is an expert K-rich, shoshonitic, and calc-alkaline magmatism of the Mediterranean region

	Mihai N Ducea ducea@arizona.edu He is an expert on Mediterranean magmatism

Vincenza Guarino
E-mail: vincenza.guarino@unina.it

Naples (Italy) - September 27, 2023

Dear Prof. Dr. Astrid Holzheid,
Editor-in-Chief of Geochemistry,

Here you can find the manuscript: “The geochemistry of leucite-bearing lavas from early stages of the Somma-Vesuvius volcanic complex: feeder systems and mantle enrichment processes in the Neapolitan district of the Roman Magmatic Province”, written by Vincenza Guarino, Roberto Solone, Martina Casalini, Luigi Franciosi, Luigi Dalla, Vincenzo Morra, Sandro Conticelli, and Leone Melluso, submitted for publication to Geochemistry.

In this manuscript, we report the first important data set related to the Somma activity. We report new and original geochemical and Sr-Nd-O isotope data of lavas and dikes collected along the entire stratigraphic log of the Somma volcano, sampling the caldera wall and the outer slopes. The data are discussed in the broader context of the petrological evolution of the Somma-Vesuvius volcanic rocks. The aim is to better elucidate the processes that led to the transition from slightly to highly silica undersaturated magmas over time. The presumed mantle-related geochemical features and the importance of Somma magmas in the RMP are also highlighted.

We are confident that the manuscript meets the quality standards of Geochemistry. We are confident that our conclusions will be of interest to a wide readership of researchers interested in this topic.

Yours sincerely,

On behalf of the other authors
Vincenza Guarino

The geochemistry of leucite-bearing lavas from early stages of the Somma-Vesuvius volcanic complex: feeder systems and mantle enrichment processes in the Neapolitan district of the Roman Magmatic Province

Vincenza Guarino[1*], Roberto Solone[1a], Martina Casalini[2], Luigi Franciosi[1], Luigi Dallai[3], Vincenzo Morra[1], Sandro Conticelli[2,4], Leone Melluso[1]

[1] Dipartimento di Scienze della Terra, dell'Ambiente e delle Risorse, Università degli Studi di Napoli Federico II, via Cintia, 21, 80126, Napoli, Italy

[2] Dipartimento di Scienze della Terra, Università degli Studi di Firenze, via Giorgio La Pira, 4, 50121, Firenze, Italy

[3] Dipartimento di Scienze della Terra, Sapienza Università di Roma, P.le Aldo Moro, 5, 00185, Roma, Italy

[4] CNR - Istituto di Geologia Ambientale e Geoingegneria, Area della Ricerca Roma-1, Strada Provinciale 35d, 9 – 00010, Montelibretti, Roma, Italy

[a] present address: Poste Italiane

*Corresponding author:
Vincenza Guarino (vincenza.guarino@unina.it), Dipartimento di Scienze della Terra, dell'Ambiente e delle Risorse, Università degli Studi di Napoli Federico II, via Cintia, 21, 80126, Napoli, Italy

Abstract

The lavas of the Monte Somma activity (early stage of the Somma-Vesuvius volcanic complex) are mildly differentiated plagioclase-clinopyroxene-olivine- ± leucite-bearing lavas (*leucite tephrites, leucite-bearing shoshonites, latites*), low in MgO, Cr and Ni, with a Sr-Nd-isotope range ($^{87}Sr/^{86}Sr$ = 0.706865-0.707861; $^{143}Nd/^{144}Nd$ = 0.51244-0.51258) overlapping that of the Vesuvian lavas late after 1638 CE (late stage of the Somma-Vesuvius volcanic complex). The differentiation is dominated by fractional crystallization of clinopyroxene, calcic plagioclase, olivine and leucite, with limited interaction with crustal rocks. Oxygen isotopes on clinopyroxene and olivine phenocrysts ($\delta^{18}O$ = 6.5-7.9 ‰) are higher than typical uncontaminated mantle magmas. However, these values are also not fully consistent with the sole open-system assimilation+fractional crystallization of a mantle-derived ultrapotassic magma. A contribution from a recycled crustal component in the mantle source is required, likely dominated by sediment-derived fluids and melts. The Somma lavas are characterized by distinctly different geochemical features compared to the mafic products of the neighboring volcanic areas (i.e., Phlegrean Fields, Procida and Ischia volcanoes), where the recycled crustal component is less pronounced.

Keywords: leucite tephrites, leucite-bearing shoshonites, leucite-free shoshonites, ultrapotassic volcanism, Somma-Vesuvius, Neapolitan district, Roman Province

1. Introduction

The Somma-Vesuvius volcanic complex is one of the best known volcanoes in the world, due to its location in a densely populated area, to its history related to the effects of several Plinian and sub-Plinian eruptions (e.g., 3800 yr. B.C. "Avellino", 79 CE "Pompeii" and 472 CE "Pollena" eruptions), one of which caused the disappearance of the cities of Pompeii, Herculaneaum and Stabiae. This volcano belongs to the Neapolitan district (Fig. 1), which is the southernmost volcanic cluster of the Roman Magmatic Province (e.g., Washington, 1906; Avanzinelli et al., 2009; Conticelli et al., 2010, 2015). The Roman Magmatic Province (RMP) occupies the Tyrrhenian side of the Apennine chain from southern Tuscany to Naples and is composed of several volcanic complexes of Pleistocene to Quaternary age that share potassic to ultrapotassic affinities (e.g., Washington, 1906; Beccaluva et al., 1991; Conticelli et al., 2010; Peccerillo, 2017). Beccaluva et al. (1991) first identified a marked geochemical and isotopic discontinuity between the Roccamonfina volcano and the southernmost parts of the RMP belonging to the Neapolitan district. This geochemical discontinuity has been interpreted as the result of a different sedimentary contribution in a slightly more enriched mantle, generally thought to be similar to the source of E-MORB (e.g., D'Antonio and Di Girolamo, 1994; D'Antonio et al., 1996, 1999; Iovine et al., 2018) and/or by the occurrence of contributions from geochemical reservoirs derived from the Aeolian subduction and from the a slab tear located in the Mt. Vulture area (e.g., Peccerillo, 2001, 2017; Avanzinelli et al., 2009, 2018; Conticelli et al., 2009, 2010, 2015). Geochemical and radiogenic isotope data indicate that the most mafic magmas of the RMP, independently of their degree of silica saturation, indicate the occurrence of subducted pelitic±carbonate lithologies in the genesis of their variably enriched mantle sources (e.g., Conticelli et al., 2002, 2007, 2013, 2015; Avanzinelli et al., 2008, 2009; Casalini et al., 2019). Recent studies have shown that recycling of sedimentary to crustal materials in subduction zones significantly modifies the Sr-Nd-O isotopes of mantle metasomatized peridotite sources (e.g., Iovine et al., 2018; Dallai et al., 2019, 2022; Avanzinelli et al., 2020; Fan et al., 2021).

The Somma-Vesuvius volcanic complex is well known for the occurrence of limestone and skarn xenoliths that well document the interaction between mantle-derived magmas and Mesozoic limestones and dolostones of the crustal basement of the volcano (e.g., Fulignati et al., 2005; Jolis et al., 2015; Balassone et al., 2013, 2023). This interaction was thought to be the main source of CO_2-bearing gases around Vesuvius. The role of the magma interaction with Mesozoic basement limestones in the genesis of the Somma-Vesuvius rocks has been historically debated (e.g., Savelli, 1967, 1968 and references therein; Di Renzo et al., 2007; Iacono Marziano et al., 2008; Conticelli et

al., 2010; Dallai et al., 2011; Pichavant et al., 2014; Jolis et al., 2015; Avanzinelli et al., 2018), and more recently also for other potassic/ultrapotassic districts of the RMP (e.g., Dallai et al., 2004; Gaeta et al., 2006, 2009; Iacono Marziano et al., 2007, 2008; Freda et al., 2008; Boari et al., 2009a, b). More recently, an important contribution of mantle-derived CO_2 to the production of Vesuvius gases has been suggested (e.g., Avanzinelli et al., 2018).

The lavas of the Mt. Somma volcanic complex have received little attention in the literature, although they constitute the largest portion of the stratovolcano. In addition, the Monte Somma volcanic rocks are characterized by fresh lavas and dikes. Geochemical and petrological data on these rocks are scarce or lacking. Indeed, previous studies of the stratovolcano have focused mainly on the explosive and effusive activity of the syn- and post-caldera Somma-Vesuvius volcano (e.g., Melluso et al., 2022 and references therein). As a corollary, the study of the complete evolution of the Somma-Vesuvius volcanic complex may provide an excellent case study to investigate in some detail the involvement of CO_2 in the early (pre-19-21 ka) activity of the Somma-Vesuvius volcanic complex.

In this paper we report new and original geochemical and Sr-Nd-O isotope data of lavas and dikes collected along the entire stratigraphic log of Mt. Somma, sampling the caldera wall and the outer slopes in extreme detail (Supplementary Figure 1). The data are discussed in the broader context of the petrological evolution of the Somma-Vesuvius volcanic rocks to better elucidate the processes that led to the transition from slightly to highly silica undersaturated magmas over time. The geochemical characteristics thought to be mantle-related, and the importance of the Somma magmas in the RMP are also highlighted.

2. Geological setting

The Somma-Vesuvius volcanic complex is located in the Neapolitan district (Fig. 2), together with the Phlegrean Fields, Procida and Ischia volcanic fields (e.g., Washington, 1906; Beccaluva et al., 1991; Avanzinelli et al., 2009; Conticelli et al., 2010, 2015), south of the Roccamonfina volcano and the buried calc-alkaline andesites found in the Parete and Castelvolturno boreholes (Beccaluva et al., 1991; Di Girolamo et al., 1996; Rouchon et al., 2008). The Somma-Vesuvius volcanic complex consists of an ancient stratovolcano, the Mt. Somma stratocone, with a summit caldera in which the younger Vesuvius Great Cone (*s.s.*) is nested. The pre-caldera summit of the Mt. Somma volcano was probably located about 500 m north of the present-day crater, at an elevation of about 1,600-1,900 m. Samples from the "Trecase 1 " geothermal well have been dated 320-360 ka, but it is highly uncertain whether these samples

belong to the Somma-Vesuvius activity (cf. Brocchini et al., 2001). The activity of Mt. Somma is earlier than the Plinian "Pomici di Base " eruption. Most of the products of the ancient Somma volcano are exposed in the inner walls of the caldera, with pyroclastic deposits found in the Camaldoli della Torre borehole (SE of the Vesuvius cone) interlayered with the products of the Campanian Ignimbrite eruption (Di Renzo et al., 2007). Three large explosive events occurred between 39 and 22 ka: the "La Schiava" eruption (36 ka), the "Taurano" eruption (36-33 ka), the "Codola" eruption (33 ka), and the “Carcavone” eruption (39-22 ka) (Sparice et al., 2017 and references therein). Other Plinian eruptions are known: the "Pomici di Base" eruption (21,670 y BP), the "Pomici Verdoline" eruption (16,130±110 yr. BP), the "Mercato" eruption (a.k.a. "Ottaviano" eruption, 8,900 yr. BP); the "Avellino" eruption (3,945±10 cal BP), the "Pompeii" eruption (79 CE) and the "Pollena" eruption (472 CE) (e.g., Melluso et al., 2022 and references therein). After minor activity just after the 472 CE and medieval activity, the last period of activity started in 1631 CE with a mild and semi-persistent activity, with minor lava effusions and short quiescent periods (last event 1944 CE). Each quiescent period was preceded by relatively powerful explosive effusive polyphase eruptions.

Tomographic images of the volcano reveal a central cylindric core of high rigidity below the axial area of the volcano (e.g., Zollo et al., 1996; Fedi et al., 2018 and references therein), which has been interpreted as a solidified magmatic intrusion or conduit. A sharp decrease in P-wave velocity is observed below 9-10 km depth; this feature is thought to be evidence for a magma reservoir (e.g., Zollo et al., 1996; Piana Agostinetti and Chiarabba, 2008).

3. Materials, methods, and classification of Mt. Somma volcanic rocks

Ninety-nine fresh lavas and five fresh dikes were collected (Fig. 2; Supplementary Figure 1) and are representative of the pre-caldera volcanic history. Analytical techniques are described in the Supplementary Material 1 (see Cucciniello et al., 2017, 2022; Guarino et al., 2021). Trace elements, determined by ICP-OES and ICP-MS, are reported in Table 1, while XRF analyses are reported in Supplementary Table 1. Detailed petrographic description, mineral chemistry, and crystallization conditions are given in Supplementary Material 2.

According to the K_2O-Na_2O diagram of Middlemost (1975), to the criteria of Foley et al. (1987) and the K_2O-SiO_2 diagram (Di Girolamo, 1984), the Somma lavas and dikes are mainly ultrapotassic rocks, leucite-bearing rocks, with subordinate potassic leucite-free rocks (Fig. 3a, b). Overall, the Somma ultrapotassic volcanic rocks are predominantly *nepheline*-normative and subordinately *leucite*-normative (Supplementary Table 1); the potassic volcanic rocks are the least

silica-undersaturated. According to the degree of silica-saturation, we divide the leucite-bearing lavas into three main groups:

(1) *Leucite tephrites* (*s.l.*): This group of rocks consists of leucite-bearing lavas with leucite both as phenocrysts and in the CIPW norm. These rocks are highly silica undersaturated (SSU) [*leucite*-normative, *leucite (lc)* = 8-22%; *nepheline (ne)* = 11-17%] with terms ranging from leucite-tephrite to leucite-tephriphonolite (Fig. 3c, d). This group is equivalent in terms of mineralogy, petrography (Supplementary Material 2.1) and chemical composition to the lavas of the recent Vesuvius Great Cone activity (1631-1944 CE).

(2) *Leucite-bearing shoshonites:* This group of rocks consists of leucite-bearing rocks without leucite in the CIPW norm. These rocks plot in the latite and shoshonite fields of the TAS and R_1R_2, with a few samples crossing the boundary with tephrites (Fig. 3c, d; Supplementary Material 2.1). Since the normative *nepheline* is variable but significantly high (2-13%), these rocks are slightly to moderately silica undersaturated (hereafter MSU).

(3) *Leucite-free shoshonites:* This group of rocks has $K_2O/Na_2O < 2$ and plots in the field of potassic series in the Na_2O-K_2O diagram and in the shoshonitic field of the K_2O-SiO_2 diagram (Fig. 3a, b; Supplementary Material 2.1). In the TAS and R_1-R_2 diagrams, these rocks plot mainly in the latite field (hereafter *latites*) (Fig. 3c, d).

The distinction between the MSU and SSU groups corresponds to a lithologic discontinuity and a marked change in slope noted along the caldera wall, where the SSU overlie the Somma lavas and dikes (Supplementary Material 2.1).

4. Major- and trace element geochemistry

The concentration of MgO in the Somma lavas and dikes ranges from 5.8 to 2.0 wt%, with Cr and Ni < 114 and < 54 ppm, respectively; the relatively low forsterite content of olivine and the low Mg# of clinopyroxene phenocrysts (Supplementary Material 2.2) indicate that none of these rocks have compositions that can be attributed to liquids in equilibrium with a mantle source. Concentrations of CaO, Al_2O_3, Na_2O, SiO_2, Sc, and V decrease with MgO, while TiO_2, Fe_2O_{3t}, P_2O_5, K_2O, and other elements have a more limited correlation (Supplementary Figure 2). These variations seem to be compatible with the removal of the observed phenocryst phases. The increase in Al_2O_3 and the decrease in CaO, Sc, and V indicate a more significant removal of clinopyroxene and magnetite than plagioclase and leucite (Supplementary Figures 2 and 3). For a given MgO, variations in major oxides and trace elements such as Zr, Sr, Y, and Nb are not fully consistent with simple fractional crystallization schemes of the observed phases (Supplementary Figure 3).

The Somma bulk rocks have a significant compositional range for fluorine (SSU group: F = 1079-2105 ppm; MSU group: F = 1046-2103 ppm; Latite group: F = 1061-1475 ppm) and chlorine (SSU group: Cl = 137-4551 ppm; MSU group: Cl = 46-1766 ppm; Latite group: Cl = 40-358 ppm), while S is significant in two SSU samples (69 and 1903 ppm) (Supplementary Figure 3). Therefore, the petrogenetic contribution of F and Cl in the petrogenesis of the Somma lavas should be considered (e.g., Melluso et al., 2022).

The chondrite normalized REE patterns of the Somma lavas and dikes are moderately LREE enriched (La_N/Yb_N = 15-27) and with significant Eu troughs [$Eu/Eu^* = Eu_N/(Sm_N \times Gd_N)^{0.5}$ = 0.8-0.9], typical of all the mafic leucite-bearing rocks of the RMP (e.g., Rogers et al., 1985; Boari et al., 2009b; Fig. 4). No significant differences are observed with increasing degree of differentiation (MgO concentration as a proxy) and group affinity, indicating that the europium (Eu) trough of the chondrite normalized patterns is not related to plagioclase removal.

The Somma lavas and dikes have Nb/Yb (11-25), Th/Yb (6-13), and Ba/Nb (37-83) ratios are significantly higher than mantle ratios, whereas the La/Nb ratio (1.4-2) is only slightly higher (Table 1 and Fig. 5). The Zr/Hf (40-50) and Nb/Ta (16-23) ratios are also slightly higher than typical mantle ratios, Nb/U is low (4-10), and Th/U (2.7-3.7) is slightly low compared to the typical mantle ratios (cf., Lyubetskaya and Korenaga, 2007). The mantle-normalized multielement patterns of the Monte Somma lavas have troughs at Nb, Ta, and Ti, a peak at Pb and generally marked Large Ion Lithophile Element (LILE) enrichment compared to HFSE (Fig. 6). Zr and Hf are not markedly depleted relative to the neighboring REE.

5. Nd, Sr, and O isotope composition of the Mt. Somma lavas

The Somma lavas have $^{87}Sr/^{86}Sr$ ranging from 0.70687 to 0.70786 and $^{143}Nd/^{144}Nd$ ranging from 0.51244 to 0.51258, with no systematic variation with the degree of magmatic differentiation (Table 2; Fig. 7). These data are consistent with known fields for Somma-Vesuvius volcanic products (e.g., 25 ka to the medieval and 1631-1944 A.D eruptions; Fig. 7), but also with products from the Neapolitan district, but formed by more differentiated rocks (i.e., trachyte). On the other hand, the Sr-Nd-isotopic ranges of Vesuvius are significantly different from the isotopic composition of the basalts of Procida (Solchiaro samples) and Ischia, which represent the most primitive volcanic products erupted in the Phlegrean-Ischian volcanic areas (Fig. 7), excluding any comagmatic origin of the mafic magmas of the different volcanic districts.

The oxygen isotope composition of the Somma-Vesuvio lavas has been studied using the $\delta^{18}O$ values of clinopyroxene. This is due to the ubiquitous occurrence of this mineral, and its chemical

and isotopic sensitivity to carbonate contamination (Dallai et al., 2004). Mineral separates from different samples have $\delta^{18}O$ values ranging from +6.3 to +7.9 ‰ (Table 2). Considering the typical fractionation between clinopyroxene and equilibrium melt compositions, this range is significantly higher than mantle-derived magmas. The negative SiO_2- $\delta^{18}O$ and Cr- $\delta^{18}O$ covariation trends of the MSU samples indicate that the overall oxygen isotope composition of clinopyroxene increased with the degree of magmatic evolution of the samples. Comparable $\delta^{18}O$ values (6.4-7.0 ‰) are obtained for the olivine separates, suggesting isotopic non-equilibrium can be envisaged with clinopyroxene (see Supplementary Figure 4a).

6. Discussion

The mildly silica undersaturated (MSU) and the leucite-free shoshonitic and latite rocks of Somma volcano do not represent just "a few outliers" as previously reported (e.g., Joron et al., 1987; Peccerillo, 2005; Santacroce et al., 2008), but rather, they form the bulk of the Mt. Somma eruptive units. Although the well-known transition to more silica undersaturated products is evident, it appears that it should not be considered as sharp as previously thought. In addition, some of the mildly silica undersaturated (MSU) rocks also have a marked distinctly "intermediate" character, unlike the other rocks. Their occurrence is never negligible or even unrecorded. These simple observations provide interesting clues for the understanding of the petrological model for the Somma-Vesuvius volcanic complex, which justifies the presence of mafic rocks with varying degrees of silica undersaturation. The Mt. Somma lavas have their counterparts in the mafic products of the "Pomici di Base" pyroclastic eruption, which range in composition from leucite shoshonite to trachyte (e.g., Landi et al., 1999; Melluso et al., 2022), and are therefore part of a slightly silica undersaturated rock suite that is not comagmatic with the rest of the Somma-Vesuvius phonolites.

6.1. Relationships between MSU, Latites (leucite-free rocks) and SSU (Vesuvius-like)

Starting with the most "primitive" compositions above, the full range of Somma epoch magmas was modeled using major element mass balance calculations (Stormer and Nicholls, 1978), and the results are summarized in Supplementary Table 2.

In the highly silica undersaturated (SSU) rocks, the major oxide transitions from the least to the most evolved lava compositions (samples MRL3 to MRL97v; *Vesuvius-like*) were adequately modeled with a maximum 42 % removal of clinopyroxene-rich leucite-gabbro (essexite) solid

(~51% clinopyroxene, ~18 % plagioclase, ~20 % leucite, ~5 % magnetite, ~3 % olivine, and ~3 % apatite; $\Sigma R^2 = 0.180$). The tested transitions between the highly silica undersaturated rocks (sample MRL18, SSU), the latite (sample MRL71), and mildly silica undersaturated rocks (sample MRL39, MSU) were modeled with 35-47 % removal of a leucite-rich extract (~46-55 % leucite, ~22-29 % clinopyroxene, ~10-14 % plagioclase, ~2-3 % olivine, ~5-7 % magnetite, and ~3-4 % apatite; $\Sigma R^2 =$ 0.097-0.239). In the MSU group, the transition from the least to the most evolved lava compositions of the mildly silica undersaturated rocks (from MRL100 or MRL27 to MRL86 samples) was adequately modeled with 21-32 % removal of similar clinopyroxene-rich leucite gabbro (essexite) solid (~43-45% clinopyroxene, ~27-38 % leucite, ~2-16 % plagioclase, ~7 % olivine, ~5-8 % magnetite, and ~0-2 % apatite; $\Sigma R^2 = 0.03$-0.08). The transition from less evolved "shoshonitic" MSU samples (i.e., MRL100 and MRL27) to more evolved latites (samples MRL103 and MRL104) is obtained by 40-56 % removal of a leucite-bearing clinopyroxenite (~37-41 % clinopyroxene, ~23-33 % leucite, ~13-21 % plagioclase, ~6-9 % olivine, ~1-3 % apatite, and ~5-7 % magnetite; at $\Sigma R^2 = 0.12$-0.18). The transition to the most evolved latites (from sample MRL69 to sample MRL104) is compatible with a 26 % removal of a clinopyroxene- and leucite-rich gabbro (~59 % plagioclase, ~25 % clinopyroxene, ~5 % leucite, ~7 % olivine, and ~3 % magnetite; $\Sigma R^2 = 0.20$). Of course, the reliability of the major element mass balance calculations reported above is not a proof of the actual occurrence of a given process; however, it is a strong indication of the reliability of processes involving the separation of phases with the chemical composition of the observed phenocrysts in an alkaline magmatic system. The amount of plagioclase removal in the different transitions is consistent with Sr being only a slightly incompatible element, since a typical K_d for bytownitic/labradoritic plagioclase is close to 2 (e.g., Bédard, 2006).

6.2. Trace element modelling

We have shown that the major and trace element variations of the most primitive magmas of each group of rocks recognized within the Mt. Somma activity cannot be produced by closed system fractional crystallization processes involving mineralogical assemblages represented by the phenocrysts (and their compositions) observed in the thin sections. The proposed models are, of course, approximations that require a closed magmatic system. Such a scenario seems oversimplified for Somma-Vesuvius, since petrographic (e.g., variably zoned plagioclase and clinopyroxene phenocrysts, the occurrence of skarn and limestone xenoliths) and petrochemical evidence (chemical disequilibrium between clinopyroxene crystals and their host bulk-rock composition, pronounced scatter of major and trace element concentrations, isotopic variability

within juvenile clasts from the same eruption) seem to suggest some open-system fractional crystallization (e.g., Santacroce, 1987; Ayuso et al., 1998; Peccerillo, 2005; Piochi et al., 2006; Di Renzo et al., 2007). The moderate variability of the Sr-Nd isotope ratios is consistent with the interaction of Somma-Vesuvius magmas with wall rock compositions that do not exhibit markedly different isotopic values, as in the case of typical Mesozoic limestones/dolostones of the Apennine chain ($^{87}Sr/^{86}Sr$ ~0.707-0.709 and $^{143}Nd/^{144}Nd$ ~0.512; Del Moro et al., 2001; Melluso et al., 2003; Fulignati et al., 2005; Piochi et al., 2006; Conticelli et al., 2009a, b; Boari et al., 2009b; Rosatelli et al., 2023), which is one of the rock types in the basement beneath the Somma-Vesuvius area (e.g., Santacroce, 1987; Brocchini et al., 2001). Although some interaction between the Somma-Vesuvius magmas and the limestone-dolostone sedimentary wall rocks certainly occurred and is seen in the skarn xenoliths, common in the pyroclastic record, the exact role of these processes in the evolution of the Somma-Vesuvius magmas is still uncertain. Two contrasting hypotheses have been proposed: i) a limited (though significant) role for limestone assimilation, subordinate to the effects of fractional crystallization of the observed phenocrysts (e.g., Savelli, 1968); ii) a dominant role for limestone assimilation, as the main process leading to the progressive increase in alkalinity and degree of silica-undersaturation of the Somma-Vesuvius magmas (Rittmann, 1933; Iacono Marziano et al., 2007).

6.3. The transition from leucite-bearing shoshonitic to leucite-tephritic magmas

Magma-carbonate interaction is a multistep process leading to the formation of the skarn shell, magmatic cumulates, and melt differentiation (e.g., Savelli, 1976). Crustal contamination of magmas can occur through assimilation of solid material (carbonate and/or skarn), and carbonate-derived CO_2 flux (Dallai et al., 2011). Melt-carbonate interaction is thought to occur on in the order of minutes, resulting in geochemical contamination of the melt coupled with intense CO_2 vesiculation at the melt-carbonate interface. In contrast, melt homogenization by physical mixing and mingling promoted by exsolving volatiles is a slower process, due to the low ability of silicate and carbonate melts to mix on a syn-eruptive timescale (Deegan et al., 2010; Jolis et al., 2013; Gozzi et al., 2014).

The chemical composition of the Somma-Vesuvius volcano shifts from the moderately silica undersaturated lavas of Mt. Somma to the highly silica undersaturated products of Vesuvius, a feature not observed in the nearby Phlegrean Fields, Procida or Ischia and exactly the opposite of what is found in the Roccamonfina volcanic complex or in the Alban Hills (e.g., Conticelli et al., 2009b and references therein; Boari et al., 2009a, b). Some authors associate the increasing degree

of silica undersaturation with increasing carbonate assimilation (e.g., Freda et al., 2008; Iacono Marziano et al., 2007; Mollo et al., 2010; Jolis et al., 2015; Carter and Dasgupta, 2016). The interaction of the magma with the basement limestone could have led to the occurrence of variably silica undersaturated rock series, starting from a single, weakly undersaturated, potassic parental magma. In particular, the model proposed by Iacono Marziano et al. (2007) for the Somma-Vesuvius suggests that the transition from the weakly undersaturated magmas of the older Somma activity to the progressively more undersaturated magmas of the following periods can be achieved by significant carbonate assimilation (up to 15-17%) accompanied by clinopyroxene removal (35-50%). However, several authors have pointed out that magma-wall rock interaction cannot involve significant mass exchange towards the magmas, arguing for a very efficient isolation of the interior of magma bodies (due to the development of a solidification front and a Ca-phases-rich skarn shell at the boundary between the crystallizing magmas and the limestone wall rocks (e.g., Savelli, 1967; Del Moro et al., 2001). On the other hand, carbonate decomposition may be responsible for a more extensive mass exchange during crust-magma interaction at the continental crustal level (e.g., Deegan et al., 2010; Mollo et al., 2010; Carter and Dasgupta, 2016). This implies that crustal contamination of magmas might could occur through assimilation of solid material (carbonate and/or skarn) rather than through crustally derived CaO-rich melt (Di Rocco et al., 2012) and carbonate-derived CO_2 flux (Dallai et al., 2011). As clearly shown by Mollo et al. (2010), the presence of a CO_2-rich fluid phase during carbonate assimilation can significantly affect partition coefficients and the redox state of carbonated systems. However, crustal contamination, and in particular carbonate contamination of potassic to ultrapotassic magmas at continental crustal level, however, may be difficult to decipher because of the occurrence of previous extreme crustal enrichment of the mantle source of ultrapotassic magmas due to subduction of crustal rocks and sediments, either carbonate-poor or carbonate-rich, which strongly modify the O-Sr-Nd-Pb isotopic composition of the source (e.g., Conticelli et al., 2015; Avanzinelli et al., 2018, 2020; Iovine et al., 2018; Dallai et al., 2019, 2022; Chen et al., 2021, 2023; Bragagni et al., 2022). Indeed, several papers have shown that either limestone or marl assimilation by a shoshonitic magma at the crustal level does not satisfy geochemical modeling to strongly produce silica undersaturated ultrapotassic rocks (e.g., Melluso et al., 2003; Boari et al., 2009a, b; Conticelli et al., 2015). In these cases, simply considering the very low incompatible element concentrations of limestones (e.g., Rb ~2-4 ppm, Zr <26 ppm, La ~15 ppm, Nd ~10 ppm, Eu ~0.38 ppm, Tb ~0.9 ppm, Th <3 ppm; e.g., Zhang et al., 2017; Rosatelli et al., 2023), the geochemical modeling of magma-crust interaction at the shallow level would result in a marked drop of incompatible element concentrations of the "hybridized" strongly silica undersaturated magma. Simple Assimilation and Fractional

Crystallization (AFC; DePaolo, 1981) models were performed to reproduce the transition from Somma-Vesuvius weakly silica undersaturated magmas to mildly and strongly silica undersaturated magmas by means of appropriate amounts of limestone assimilation. Trace element and isotope modeling failed to reproduce such a transition, even with different contaminants, such as marls and limestones belonging to the Apennine chain (Supplementary Figure 4b, c).

In summary, the above evidence and modeling indicate that the process of limestone assimilation was active throughout the magmatic evolution of the Somma-Vesuvius complex, but it is not able to justify the observed temporal increase in the degree of alkalinity and silica undersaturation of these magmas, also considering the variations of $\delta^{18}O$ in the Somma (and Vesuvius) magmas and the isotopic differences between ultrapotassic alkaline magmas and sedimentary limestones/dolostones or marlstones (e.g., Dallai et al., 2019; Fan et al., 2021; Rosatelli et al., 2023).

6.4. The mantle sources of the Somma-Vesuvius magmatism in the southern part of the Roman Magmatic Province

It is widely accepted that the primary magmas of the RMP are generated by partial melting of a mantle source recently enriched in potassium and related elements by subduction processes involving continental crustal material (e.g., Beccaluva et al., 1991; Peccerillo, 1998, 2017; Conticelli et al., 2002, 2011, 2015; Avanzinelli et al., 2008; Mazzeo et al., 2014; Iovine et al., 2018; Casalini et al., 2019). The relative roles of subducted sedimentary material in a variably enriched lithospheric upper mantle and shallow crustal contamination en route to the surface are still debated. The typical LILE and Pb enrichments and the troughs at Nb, Ta, and Ti observed in the most primitive mantle-normalized diagrams for the Monte Somma lavas are shared with other Roman rocks, although the Somma volcanic rocks have intermediate characteristics between the leucite-bearing volcanic rocks of the Latian district and those of Monte Vulture (e.g., Avanzinelli et al., 2009; Conticelli et al., 2015). The mafic terms of the Somma-Vesuvius and other volcanoes of the Campanian Plain have lower HFSE fractionation than Th, U and LILE compared to the leucite-bearing mafic magmas of the Latian districts of the Roman Province (e.g., Beccaluva et al., 1991; Ayuso et al., 1998; D'Antonio et al., 1999; Peccerillo, 2001; Di Renzo et al., 2007; Avanzinelli et al., 2008; Conticelli et al., 2009a; Mazzeo et al., 2014).

It is long known that the extent of the Eu troughs in the REE chondrite normalized diagrams of the mafic ultrapotassic, leucite-bearing rocks of the RMP is a feature largely inherited from the mantle source, rather than due to calcic plagioclase removal (e.g., Rogers et al., 1985), and the Mt.

Somma lavas (and the Vesuvius analogues) are no exception. The source of the RMP rocks has marked affinities with sedimentary rocks (pelites with carbonates/marls), and indeed the addition of pelitic sedimentary rocks (or melts derived from them) in a peridotite matrix could be one of the causes of the geochemical patterns of the RMP and hence of Somma-Vesuvius. To test this hypothesis, we have used a comprehensive data set of the Italian volcanic rocks south of the Alban Hills, together with the composition of typical Atlantic and Tyrrhenian Sea MORBs, within plate basalts, and sedimentary rocks of closed areas, thought to be representative of the subducted material potentially downdragged during the Cenozoic collisional events of this area of the Apennine chain. The Nb/Yb vs. Th/Yb and Nb vs. Nb/U plots point out significant differences between the regional geochemistry of MORB and within-plate mafic rocks, and that of Somma and the other volcanic rocks of the southern RMP (Fig. 5a, b). The shift to high Th/Yb and lower Nb/U compared to the MORB-WPB array indicates a differential enrichment in Th and U, at different Nb concentrations, which may be related to the degree of "within-plate" enrichment. The latter indicates the effect of fractional crystallization, but also the degree of HFSE enrichment in the mantle source, which is highest for alkaline WPB around the RMP, such as Pietre Nere, Capo Passero (Avanzinelli et al., 2012; Mazzeo et al., 2018), Cretaceous within-plate lamprophyres of the Apennine chain (Stoppa et al., 2014), and other within plate potassic or sodic provinces (such as Madagascar, Virunga, and southeastern Brazil). The mafic rocks of Ischia, Procida, Phlegrean Fields, and Somma-Vesuvius, although having a markedly distinct composition, are also different from the rocks of the potassic-ultrapotassic volcanic rocks from Roccamonfina to the Alban Hills. There is another interesting aspect related to the different genesis and geochemistry of the Pre-Miocene Apennine magmatism and the post-Miocene magmatism of the Tyrrhenian Sea margin, which implies that the K-enrichment of the sources is recent and not related to older (i.e., Hercynian, Late Paleozoic) collisional event (e.g., Gaeta et al., 2016), where also potassic silica-undersaturated magmatism is exceedingly rare. The La/Nb vs. Ba/Nb and La_N/Yb_N vs. Ba/Nb plots highlight that the mafic rocks of the Campanian district plot differently from the rest of the RMP rocks, being displaced at higher Ba/Nb for a given La/Nb (Fig. 5c, d). The shift almost disappears when the REE fractionation is considered, with only the composition of MORB and WPB being significantly different.

The Zr/Nb vs. Nb/U and Zr/Nb vs. Th/U plots also highlight peculiar aspects of the selective elemental enrichment of the Italian volcanic rocks (Fig. 5e, f): the displacement of the potassic-ultrapotassic rocks from the MORB-WPB trend is the largest at high Zr/Hf, with the largest U enrichment found in the Alban Hills, Roccamonfina and Middle Latin Valley, and the markedly higher Th/U ratios of the Roccamonfina, Alban Hills and Middle Latin Valley rocks compared to

those of the Campanian volcanoes, including Somma-Vesuvius. The type of sediment addition provides evidence that adding bulk compositions of the sedimentary rocks (e.g., Klaver et al., 2015; Balassone et al., 2016; Zhang et al., 2017; Woelki et al., 2018) are not in the highest Ba/Nb and La/Nb field of the diagrams and thus do not fully reproduce the trend, suggesting that sediment-derived fluids and melts, rather than direct sediment addition, were the components that metasomatized the mantle source and imparted the potassic/ultrapotassic signature to the magmas. Compared to other silica-undersaturated ultrapotassic magmas of the Latian district, those of Somma-Vesuvius and those of the other Neapolitan volcanoes have significantly lower $^{87}Sr/^{86}Sr$, and higher $^{143}Nd/^{144}Nd$ and $^{206}Pb/^{204}Pb$ (e.g., Conticelli et al., 2002, 2007, 2010a, b, 2015 and references therein; Di Renzo et al., 2007). In turn, the peculiar composition of the radiogenic isotope systematics is again attributed to the recycling of carbonate-bearing crustal materials (e.g., Avanzinelli et al., 2009; Conticelli et al., 2010, 2015). The involvement of such materials has been demonstrated by cross-checking different geochemical tools. The evidence provided by U-series and non-traditional stable isotopes (Mo and U) suggests that although limestone assimilation could potentially occur and influence major element concentrations, the same process is not able to significantly affect the isotopic composition and the elemental abundances of Vesuvius rocks (Avanzinelli et al., 2018; Casalini et al., 2019). On the other hand, partial melting experiments on carbonate-rich sediments at subarc conditions (P-T) may indicate that the stabilization of phases, such as epidote, influences the geochemical budget of the mantle source and, consequently, of subduction-derived products (e.g., Skora et al., 2015). In the case of Somma-Vesuvius, the presence of residual epidote during the partial melting of subducted Ca-rich sediments could explain the formation of magmas enriched in U over Th (but also in the relative proportions of other trace elements, such as Ce and Mo) and with the typical signature of both radiogenic and stable isotopes (i.e., ^{238}U-excess, $\delta^{238}U$, $\delta^{98}Mo$; Avanzinelli et al., 2018; Casalini et al., 2019). In this context, the lithological control of the metasediments involved in the ultimate petrogenesis of the magmas in the southern part of the RMP is an important parameter to consider.

The geochemical and isotopic comparison of the Somma lavas with the mafic products of the neighboring volcanoes (the Solchiaro basalts of Procida, the Grotta di Terra dyke and Arso lava, and the Zaro mafic inclusions of Ischia) is reported in the Figs. 4, 6 and 7. Two main aspects are highlighted: (1) the imprint of crustal materials in the mantle source of the Ischian and Phlegrean magmas is much less pronounced than in the source of the Mt. Somma magmas; (2) the mantle sources of the Campanian volcanic district are to be considered isotopically and geochemically heterogeneous and only generally the result of the same petrogenetic processes in a post-collisional tectonic setting.

7. Conclusions

The Mt. Somma stratocone is characterized by dominant lavas of leucite-bearing to shoshonite composition, significantly less silica undersaturated than the recent Vesuvius (*s.s.*) Great Cone analogues at the same level of differentiation and characterized by a generally evolved composition. The petrographic differences observed in the magma groups are not reflected in the geochemistry and Sr-Nd-O isotopic compositions, which overlap. Crustal contamination en route to the surface, in particular interaction with the carbonate lithologies beneath Somma-Vesuvius, is shown to be widespread in the skarn xenoliths occurring in the Vesuvius (*s.s.*) volcanic rocks, but the subduction-related trace element signature of the Somma lavas (as well as the younger Vesuvius lavas) argues for a dominant role of deep sedimentary contamination in the mantle source prior to partial melting. This is a geologically recent feature acquired in a moderately enriched mantle source, more limited in extent when compared to the strongly sediment-modified mantle in the Latian districts of the northern Roman Magmatic Province. The leucite-bearing Somma lavas have very little in common with the rocks belonging to the neighboring volcanic areas (Ischia, Procida and Phlegrean Fields), confirming once again the peculiar characteristics of the independent feeding systems, liquid descent lines and periods of activity.

Acknowledgements

This manuscript is dedicated to the memory of Prof. Pio Di Girolamo, for his never-ending passion for the rocks of Somma-Vesuvius and for his precious teaching on the genesis of Italian potassic and ultrapotassic magmas. We are particularly grateful to Lorenzo Fedele for his help in the study of these samples, and to Ciro Cucciniello for the XRF analyses and useful advice. Mariano Mercurio helped with the collection of samples during his MSc thesis. Fabio Mazzeo, Pietro Armienti and Giancarlo Serri are also in our souls. Sergio Bravi patiently prepared polished thin sections. This work was supported by MIUR 2015 grants to LM and SC (grants # 20158A9CBM, 20224T2JF4) and by MIUR 2017 grant to Ciro Cucciniello (grant # 20178LPCPW_004) and Fondi Ricerca Dipartimentale 2023 to L.M.

References

Anders, E., Grevesse, N., 1989. Abundances of the elements: Meteoritic and solar. Geochim. Cosmochim. Acta 53, 197–214.

Arevalo, R., McDonough, W.F., 2010. Chemical variations and regional diversity observed in MORB. Chem. Geol. 271, 70–85.

Avanzinelli, R., Elliott, T., Tommasini, S., Conticelli, S., 2008. Constraints on the genesis of the potassium-rich Italian volcanics from U/Th disequilibrium. J. Petrol. 49, 195–223.

Avanzinelli, R., Lustrino, M., Mattei, M., Melluso, L., Conticelli, S., 2009. Potassic and ultrapotassic magmatism in the circum-Tyrrhenian region: the role of carbonated pelitic vs. pelitic sediment recycling at destructive plate margin. Lithos 113, 213–227.

Avanzinelli, R., Sapienza, G.T., Conticelli, S., 2012. The Cretaceous to Paleogene within-plate magmatism of Pachino-Capo Passero (southeastern Sicily) and Adria (La Queglia and Pietre Nere, southern Italy): geochemical and isotopic evidence against a plume-related origin of circum-Mediterranean magmas. Eur. J. Mineral. 24, 73–96.

Avanzinelli, R., Casalini, M., Elliott, T., Conticelli, S., 2018. Carbon fluxes from subducted carbonates revealed by uranium excess at Mount Vesuvius, Italy. Geology 46, 259–262. https://doi.org/10.1130/G39766.1.

Avanzinelli, R., Bianchini, G., Tiepolo, M., Jasim, A., Natali, C., Braschi, E., Beccaluva L. Conticelli, S., 2020. Subduction-related hybridization of the lithospheric mantle revealed by trace element and Sr-Nd-Pb isotopic data in composite xenoliths from Tallante (Betic Cordillera, Spain). Lithos 352, 105316.

Ayuso, A.R., De Vivo, B., Rolandi, G., Seal, R.R., Paone, A., 1998. Geochemical and isotopic (Nd-Pb-Sr-O) variations bearing on the genesis of volcanic rocks from Vesuvius, Italy. J. Volcanol. Geotherm. Res. 82, 53–78.

Balassone, G., Scordari, F., Lacalamita, M., Schingaro, E., Mormone, A., Piochi, M., Petti C., Mondillo N., 2013. Trioctahedral micas in xenolithic ejecta from recent volcanism of the Somma-Vesuvius (Italy): Crystal chemistry and genetic inferences. Lithos 160, 84–97.

Balassone, G., Aiello, G., Barra, D., Cappelletti, P., De Bonis, A., Donadio, C., Guida, M., Melluso, L., Morra, V., Parisi, R., Pennetta, M., Siciliano, A., 2016. Effects of anthropogenic activities in a Mediterranean coastland: the case study of the Falerno-Domitio littoral in Campania, Tyrrhenian Sea (southern Italy). Mar. Pollut. Bull. 112, 271–290.

Balassone, G., Schingaro, E., Lacalamita, M., Mesto, E., Mormone, A., Piochi, M., Guarino, V., Pellino, A., D'Orazio, L., 2023. Genetic implications, composition, and structure of

trioctahedral micas in xenoliths related to Plinian eruptions from the Somma-Vesuvius volcano (Italy). Am. Mineral., *in press*, doi: 10.2138/am-2022-8782.

Beccaluva, L., Bonatti, E., Dupuy, C., Ferrara, G., Innocenti, F., Lucchini, F., Macera, P., Petrini, R., Rossi, P.L., Serri, G., Seyler, M., Siena, F., 1990. Geochemistry and mineralogy of volcanic rocks from ODP sites 650, 651, 655 and 654 in the Tyrrhenian Sea. In: Proceedings of the Ocean Drilling Program Scientific Results 107, 49–74.

Beccaluva, L., Di Girolamo, P., Serri, G., 1991. Petrogenesis and tectonic setting of the Roman Volcanic Province, Italy. Lithos 26, 191–221.

Beccaluva, L., Coltorti, M., Di Girolamo, P., Melluso, L., Milani, L., Morra, V., Siena, F., 2002. Petrogenesis and evolution of Mt. Vulture alkaline volcanism (Southern Italy). Mineral. Petrol. 74, 277–297.

Bedard, J.H., 2006. Trace element partitioning in plagioclase feldspar. Geochim. Cosmochim. Acta 70, 3717–3742.

Belkin, H. E., Kilburn, C.R., de Vivo, B., 1993. Sampling and major element chemistry of the recent (AD 1631–1944) Vesuvius activity. J. Volcanol. Geotherm. Res. 58 (1-4), 273–290.

Boari, E., Avanzinelli, R., Melluso, L., Giordano, G., Mattei, M., De Benedetti, A.A., Morra, V., Conticelli, S., 2009a. Isotope geochemistry (Sr–Nd–Pb) and petrogenesis of leucite-bearing volcanic rocks from "Colli Albani" volcano, Roman Magmatic Province, Central Italy: inferences on volcano evolution and magma genesis. Bull. Volcanol. 71, 977–1005.

Boari, E., Tommasini, S., Laurenzi, M.A., Conticelli, S., 2009b. Transition from ultrapotassic kamafugitic to sub-alkaline magmas: Sr, Nd, and Pb isotope, trace element and ^{40}Ar-^{39}Ar age data from the Middle Latin Valley volcanic field, Roman Magmatic Province, Central Italy. J. Petrol. 50, 1327–1357.

Bragagni, A., Mastroianni, F., Münker, C., Conticelli, S., Avanzinelli, R., 2022. A carbon-rich lithospheric mantle as a source for the large CO_2 emissions of Etna volcano (Italy). Geology 50, 486–490.

Brocchini, D., Principe, C., Castradori, D., Laurenzi, M.A., Gorla, L., 2001. Quaternary evolution of the southern sector of the Campanian Plain and early Somma-Vesuvius activity: insights from the Trecase I well. Mineral. Petrol. 73, 67–91.

Carter, L.B., Dasgupta, R., 2016. Effect of melt composition on crustal carbonate assimilation: Implications for the transition from calcite consumption to skarnification and associated CO_2 degassing. Geochem. Geophys. Geosyst. 17 (10), 3893–3916.

Casalini, M., Heumann, A., Marchionni, S., Conticelli, S., Avanzinelli, R., Tommasini, S., 2018. Inverse modelling to unravel the radiogenic isotope signature of mantle sources from

evolved magmas: the case-study of Ischia volcano. Ital. J. Geosci. 137, https://doi.org/:10.3301/IJG.2018.05.

Casalini, M., Avanzinelli, R., Tommasini, S., Elliott, T., Conticelli, S., 2019. Ce/Mo and molybdenum isotope systematics in subduction-related orogenic potassic magmas of central-southern Italy. Geochem. Geophys. Geosystems 20, 2753–2768.

Chen, L. M., Song, X.Y., Hu, R.Z., Yu, S.Y., Yi, J.N., Kang, J., Huang, K.J., 2021. Mg–Sr–Nd isotopic insights into Petrogenesis of the Xiarihamu mafic–ultramafic intrusion, northern Tibetan plateau, China. J. Petrol. 62 (2), egaa113.Chen, M., Boyle, E. A., Jiang, S., Liu, Q., Zhang, J., Wang, X., Zhou, K., 2023. Dissolved lead (Pb) concentrations and Pb isotope ratios along the East China Sea and Kuroshio transect—evidence for isopycnal transport and particle exchange. J. Geophys. Res. Oceans 128 (2), e2022JC019423.

Cioni, R., Marianelli, P., Santacroce, R., 1998. Thermal and compositional evolution of the shallow magma chambers of Vesuvius: evidence from pyroxene phenocrysts and melt inclusions. J. Geophys. Res. Solid Earth 103(B8), 18277–18294.

Conticelli, S., Francalanci, L., Manetti, P., Cioni, R., Sbrana, A., 1997. Petrology and geochemistry of the ultrapotassic rocks from the Sabatini Volcanic District, Central Italy: the role of evolutionary processes in the genesis of variably enriched alkaline magmas. J. Volcanol. Geotherm. Res. 75, 107–136.

Conticelli, S., D'Antonio, M., Pinarelli, L., Civetta, L., 2002. Source contamination and mantle heterogeneity in the genesis of Italian potassic and ultrapotassic volcanic rocks: Sr-Nd-Pb isotope data from Roman Province and Southern Tuscany. Mineral. Petrol. 74, 189–222.

Conticelli, S., Carlson, R.W., Widom, E., Serri, G., 2007. Chemical and isotopic composition (Os, Pb, Nd, and Sr) of Neogene to Quaternary calc-alkalic, shoshonitic, and ultrapotassic mafic rocks from the Italian peninsula: Inferences on the nature of their mantle sources. G.S.A. Special Papers 'Cenozoic Volcanism in the Mediterranean Area' 418, 171. https://doi.org/10.1130/2007.2418(09)

Conticelli, S., Guarnieri, L., Farinelli, A., Mattei, M., Avanzinelli, R., Bianchini, G., Boari, E., Tommasini, S., Tiepolo, M., Prelévic, D., Venturelli, G., 2009a. Trace elements and Sr-Nd-Pb isotopes of K-rich to shoshonitic and calc-alkalic magmatism of the Western Mediterranean region: genesis of ultrapotassic to calc-alkalic magmatic associations in post-collisional geodynamic setting. Lithos 107, 68–92.

Conticelli, S., Marchionni, S., Rosa, D., Giordano, G., Boari, E., Avanzinelli, R., 2009b. Shoshonite and sub-alkaline magmas from an ultrapotassic volcano: Sr-Nd-Pb isotope data on the

Roccamonfina volcanic rocks, Roman Magmatic Province, Southern Italy. Contrib. Mineral. Petrol. 157, 41–63.

Conticelli, S., Laurenzi, M.A., Giordano, G., Mattei, M., Avanzinelli, R., Melluso, L., Tommasini, S., Boari, E., Cifelli, F., Perini, G., 2010. Leucite-bearing (kamafugitic/leucititic) and-free (lamproitic) ultrapotassic rocks and associated shoshonites from Italy: constraints on petrogenesis and geodynamics. J. Virtual Explor. 36 (20), 1–95.

Conticelli, S., Avanzinelli, R., Marchionni, S., Tommasini, S., Melluso, L., 2011. Sr-Nd-Pb isotopes from the Radicofani Volcano, Central Italy: constraints on heterogeneities in a veined mantle responsible for the shift from ultrapotassic shoshonite to basaltic andesite magmas in a post-collisional setting. Mineral. Petrol. 103, 123–148.

Conticelli, S., Avanzinelli, R., Poli, G., Braschi, E., Giordano, G., 2013. Shift from lamproite-like to leucititic rocks: Sr–Nd–Pb isotope data from the Monte Cimino volcanic complex vs. the Vico stratovolcano, Central Italy. Chem. Geol. 353, 246–266.

Conticelli, S., Avanzinelli, R., Ammannati, E., Casalini, M., 2015. The role of carbon from recycled sediments in the origin of ultrapotassic igneous rocks in the Central Mediterranean. Lithos 232, 174–196.

Cucciniello, C., Melluso, L., le Roex, A.P., Jourdan, F., Morra, V., de' Gennaro, R., Grifa, C., 2017. From nephelinite, basanite and basalt to peralkaline trachyphonolite and comendite in the Ankaratra volcanic complex, Madagascar: $^{40}Ar/^{39}Ar$ ages, phase compositions and bulk-rock geochemical and isotopic evolution. Lithos 274–275, 363–382.

Cucciniello, C., Avanzinelli, R., Sheth, H.C., Casalini, M., 2022. Mantle and crustal contributions to the Mount Girnar alkaline plutonic complex and the circum-Girnar mafic-silicic intrusions of Saurashtra, northwestern Deccan Traps. J. Petrol. 63, egac007.

D'Antonio, M., Di Girolamo, P., 1994. Petrological and geochemical study of mafic shoshonitic volcanics from Procida-Vivara and Ventotene Islands (Campanian Region, South Italy). Acta Vulcanol. 5, 69–80.

D'Antonio, M., Tilton, G.R., Civetta, L., 1996. Petrogenesis of Italian alkaline lavas deduced from Pb-Sr-Nd isotope relationships. In: Basu, A., Hart, S.R. (eds.), Earth Processes: Reading the Isotopic Code, Washington D.C., American Geophysical Union Monograph Series 95, 253–267.

D'Antonio, M., Civetta, L., Di Girolamo, P., 1999. Mantle source heterogeneity in the Campanian Region (South Italy) as inferred from geochemical and isotopic features of mafic volcanic rocks with shoshonitic affinity. Mineral. Petrol. 67, 163–192.

D'Antonio, M., Tonarini, S., Arienzo, I., Civetta L., Di Renzo, V., 2007. Components and processes in the magma genesis of the Phlegrean Volcanic District, southern Italy. In: Beccaluva, L., Bianchini, G., Wilson, M. (eds.), Cenozoic volcanism in the Mediterranean area. Geol. Soc. Am. Spec. Pap. 418, 203–220.

Dallai, L., Freda, C., Gaeta, M., 2004. Oxygen isotope geochemistry of pyroclastic clinopyroxene monitors carbonate contributions to Roman-type ultrapotassic magma. Contrib. Mineral. Petrol. 148, 247–263.

Dallai, L., Cioni, R., Boschi, C., D'Oriano, C., 2011. Carbonate-derived CO_2 purging magma at depth: influence on the eruptive activity of Somma-Vesuvius, Italy. Earth Planet. Sci. Lett. 310, 84–95.

Dallai, L., Bianchini, G., Avanzinelli, R., Natali, C., Conticelli, S., 2019. Heavy oxygen recycled into the lithospheric mantle. Sci. Rep. 9, 8793.

Dallai, L., Bianchini, G., Avanzinelli, R., Deloule, E., Natali, C., Gaeta, M., Cavallo, A., Conticelli, S., 2022. Quartz-bearing rhyolitic melts in the Earth's mantle. Nat. Commun. 13 (1), 7765.

De Astis, G., Kempton, P.D., Peccerillo, A., Wu, T.W., 2006. Trace element and isotopic variations from Mt. Vulture to Campanian volcanoes: constraints for slab detachment and mantle inflow beneath southern Italy. Contrib. Mineral. Petrol. 151, 331–351.

de La Roche, H., Leterrier, P., Grandclaude, P., Marchal, E., 1980. A classification of volcanic and plutonic rocks using R_1-R_2 diagram and major element analyses. Its relationships with current nomenclature. Chem. Geol. 29, 183–210.

Del Moro, A., Fulignati, P., Marianelli, P., Sbrana, A., 2001. Magma contamination by direct wall rock interaction: constraints from xenoliths from the walls of a carbonate-hosted magma chamber (Vesuvius 1944 eruption). J. Volcanol. Geotherm. Res. 112, 15–24.

DePaolo, D.J., 1981. Trace element and isotopic effects of combined wall rock assimilation and fractional crystallization. Earth Planet. Sci. Lett.53, 189–202.

Di Girolamo, P., 1984. Magmatic character and geotectonic setting of some Tertiary-Quaternary Italian volcanic rocks: orogenic, anorogenic and "transitional" associations – a review. Bull. Volcanol. 47, 421–432.

Di Girolamo, P., Franciosi, L., Melluso, L., Morra, V., 1996. The calc-alkaline rocks of the Campanian plain: new mineral chemical data and possible link with acidic rocks of the Pontine Island. Period. Mineral. 65, 305–316.

Di Renzo, V., Di Vito, M.A., Arienzo, I., Carandente, A., Civetta, L., D'Antonio, M., Giordano, F., Orsi, G., Tonarini, S., 2007. Magmatic history of Somma-Vesuvius on the basis of new

geochemical and isotopic data from deep borehole (Camaldoli della Torre). J. Petrol. 48, 753–784.

Di Rocco, T., Freda, C., Gaeta, M., Mollo, S., Dallai, L., 2012. Magma chambers emplaced in carbonate substrate: petrogenesis of skarn and cumulate rocks and implications for CO_2 degassing in volcanic areas. J. Petrol. 53 (11), 2307–2332.

Fan, W., Jiang, N., Hu, J., Liu, D., Zhao, L., Li, T., 2021. A metasomatized ^{18}O-rich veined lithospheric mantle source for ultrapotassic magmas. Lithos 382–383, 105964.

Fedele, L., Scarpati, C., Lanphere, M., Melluso, L., Morra, V., Perrotta, A., Ricci, G., 2008. The Breccia Museo formation, Campi Flegrei, southern Italy: geochronology, chemostratigraphy and relationship with the Campanian Ignimbrite eruption. Bull. Volcanol. 70, 1189–1219.

Fedi, M., Cella, F., D'Antonio, M., Florio, G., Paoletti, V., Morra, V., 2018. Gravity modelling finds a large magma body in the deep crust below the Gulf of Naples, Italy. Sci. Rep. 8, 8229.

Foley, S., Venturelli, G., Green, D.H., Toscani, L., 1987. The ultrapotassic rocks: characteristics, classification, and constraints for petrogenetic models. Earth-Sci. Rev. 24 (2), 81–134.

Freda, C., Gaeta, M., Misiti, V., Mollo, S., Dolfi, D., Scarlato, P., 2008. Magma-carbonate interaction: an experimental study on ultrapotassic rocks from Alban Hills (Central Italy). Lithos 101, 397–415.

Fulignati, P., Panichi, C., Sbrana, A., Caliro, S., Gioncada, A., Del Moro, A., 2005. Skarn formation at the walls of the 79AD magma chamber of Vesuvius (Italy): mineralogical and isotopic constraints. N. Jb. Miner. Abh. 181, 53–66.

Gaeta, M., Freda, C., Christensen, J.N., Dallai, L., Marra, F., Karner, D.B., Scarlato, P., 2006. Time-dependent geochemistry of clinopyroxene from the Alban Hills (Central Italy): clues to the source and evolution of ultrapotassic magmas. Lithos 86 (3–4), 330–346.

Gaeta, M., Di Rocco, T., Freda, C., 2009. Carbonate assimilation in open magmatic systems: the role of melt-bearing skarns and cumulate-forming processes. J. Petrol. 50(2), 361–385.

Gaeta, M., Freda, C., Marra, F., Arienzo, I., Gozzi, F., Jicha, B., Di Rocco, T., 2016. Paleozoic metasomatism at the origin of Mediterranean ultrapotassic magmas: constraints from time-dependent geochemistry of Colli Albani volcanic products (Central Italy). Lithos 244, 151–164.

Gozzi, F., Gaeta, M., Freda, C., Mollo, S., Di Rocco, T., Marra, F., Dallai, L., Pack, A., 2014. Primary magmatic calcite reveals origin from crustal carbonate. Lithos 190, 191–203.

Guarino, V., Wu, F.-Y., Lustrino, M., Melluso, L., Brotzu, P., Gomes, C.B., Ruberti, E., Tassinari, C.C.G., Svisero, D.P., 2013. U-Pb ages, Sr-Nd- isotope geochemistry and petrogenesis of

kimberlites, kamafugites and phlogopite-picrites of the Alto Paranaíba Igneous Province, Brazil. Chem. Geol. 353, 65–82.

Guarino, V., Lustrino, M., Zanetti, A., Ruberti, E., Tassinari, C.C.G., de' Gennaro, R., Melluso, L., 2021. Mineralogy and geochemistry of a giant agpaitic magma reservoir: the Late Cretaceous Poços de Caldas potassic alkaline complex (SE Brazil). Lithos 398–399, 106330.

Iacono Marziano, G., Gaillard, F., Pichavant, M., 2007. Limestone assimilation and the origin of CO_2 emissions at the Alban Hills (Central Italy): Constraints from experimental petrology. J. Volcanol. Geotherm. Res. 166(2), 91–105.

Iacono Marziano, G., Gaillard, F., Pichavant, M., 2008. Limestone assimilation by basaltic magmas: an experimental re-assessment and application to Italian volcanoes. Contrib. Mineral. Petrol. 155, 719–738.

Iovine, R.S., Mazzeo, F.C., Wörner, G., Pelullo, C., Cirillo, G., Arienzo, I., Pack, A., D'Antonio, M., 2018. Coupled $\delta^{18}O$- $\delta^{17}O$ and $^{87}Sr/^{86}Sr$ isotope compositions suggest a radiogenic and ^{18}O-enriched magma source for Neapolitan volcanoes. Lithos 316–317, 199–211.

Jolis, E.M., Freda, C., Troll, V.R., Deegan, F.M., Blythe, L.S., McLeod, C.L., Davidson, J.P., 2013. Experimental simulation of magma–carbonate interaction beneath Mt. Vesuvius, Italy. Contrib. Mineral. Petrol. 166, 1335–1353.

Jolis, E.M., Troll, V.R., Harris, C., Freda, C., Gaeta, M., Orsi, G., Siebe, C., 2015. Skarn xenolith record crustal CO_2 liberation during Pompeii and Pollena eruptions, Vesuvius volcanic system, central Italy. Chem. Geol. 415, 17–36.

Joron, J.L., Metrich, N., Rosi, M., Santacroce, R., Sbrana, A., 1987. Chemistry and Petrography. In: "Somma Vesuvius", Santacroce R. (Ed.), C.N.R. Quaderni de "La Ricerca Scientifica", 8, 105–174.

Klaver, M., Djuly, T., de Graaf, S., Sakes, A., Wijbrans, J.R., Davies, G., Vroon, P.Z., 2015. Temporal and spatial variations in provenance of Eastern Mediterranean Sea sediments: implications for Aegean and Aeolian arc volcanism. Geochim. Cosmochim. Acta 153, 149–168.

Landi, P., Bertagnini, A., Rosi, M., 1999. Chemical zoning and crystallization mechanism in the magma chamber of the Pomici di Base plinian eruption of Somma-Vesuvius (Italy). Contrib. Mineral. Petrol. 135, 179–197.

Lustrino, M., Cucciniello, C., Melluso, L., Tassinari, C.C.G., de' Gennaro, R., Serracino, M., 2012. Petrogenesis of Cenozoic volcanic rocks in the NW sector of the Gharyan volcanic field, Libya. Lithos 155, 218–235.

Lyubetskaya, T., Korenaga, J., 2007. Chemical composition of Earth's primitive mantle and its variance: 1. methods and results. J. Geophys. Res. 112, B03211. doi: 10.1019/2005JB004223.

Marianelli, P., Métrich, N., Sbrana, A., 1999. Shallow and deep reservoirs involved in magma supply of the 1944 eruption of Vesuvius. Bull. Volcanol. 61, 48–63.

Mazzeo, F.C., D'Antonio, M., Arienzo, I., Aulinas, M., Di Renzo, V., Gimeno, D., 2014. Subduction-related enrichment of the Neapolitan volcanoes (Southern Italy) mantle source: new constraints on the characteristics of the slab-derived components. Chem. Geol. 386, 165–183.

Mazzeo, F.C., Arienzo, I., Aulinas, M., Casalini, M., Di Renzo, V., D'Antonio, M., 2018. Mineralogical, geochemical and isotopic characteristics of alkaline mafic igneous rocks from Punta delle Pietre Nere (Gargano, southern Italy). Lithos 308–309, 316–328.

Melluso, L., Conticelli, S., D'Antonio, M., Mirco, N. P., Saccani, E., 2003. Petrology and mineralogy of wollastonite-and melilite-bearing paralavas from the Central Apennines, Italy. Am. Mineral. 88 (8–9), 1287–1299.

Melluso, L., de' Gennaro, R., Fedele, L., Franciosi, L., Morra, V., 2012. Evidence of crystallization in residual, Cl–F–rich, agpaitic, trachyphonolitic magmas and primitive Mg-rich basalt-trachyphonolite interaction in the lava domes of the Phlegrean Fields (Italy). Geol. Mag. 149(3), 532–550.

Melluso, L., Morra, V., Guarino, V., de' Gennaro, R., Franciosi, L., Grifa, C., 2014. The crystallization of shoshonitic to peralkaline trachyphonolitic magmas in a H_2O-Cl-F- rich environment at Ischia (Italy), with implications for the feeder system of the Campania Plain volcanoes. Lithos 210–211, 242–259.

Melluso, L., Cucciniello, C., le Roex, A.P., Morra, V., 2016. The geochemistry of primitive volcanic rocks of the Ankaratra volcanic complex, and source enrichment processes in the genesis of the Cenozoic magmatism in Madagascar. Geochim. Cosmochim. Acta 185, 435–452.

Melluso, L., Scarpati, C., Zanetti, A., Sparice, D., de' Gennaro, R., 2022. The petrology and geochemistry of zoned, phonolitic Plinian and sub-Plinian eruptions of Somma-Vesuvius, Italy: role of accessory phase removal, independently filled magma reservoirs with time, and transition from slightly to highly silica undersaturated series in an ultrapotassic stratovolcano. Lithos 430–431, 106854.

Middlemost, E.A.K., 1975. The basalt clan. Earth-Sci. Rev. 11, 337–364.

Mollo, S., Del Gaudio, P., Ventura, G., Iezzi, G., Scarlato, P., 2010. Dependence of clinopyroxene composition on cooling rate in basaltic magmas: Implications for thermobarometry. Lithos 118 (3–4), 302–312.

Pappalardo, L., Piochi, M., D'Antonio, M., Civetta, L., Petrini, R., 2002. Evidence for multi-stage magmatic evolution during the past 60 kyr at Campi Flegrei (Italy) deduced from Sr, Nd and Pb isotope data. J. Petrol. 43 (8), 1415–1434.

Pappalardo, L., Piochi, M., D'Antonio, M., Civetta, L., Petrini, R., 2002. Evidence for multi-stage magmatic evolution during the past 60 kyr at Campi Flegrei (Italy) deduced from Sr, Nd and Pb isotope data. J. Petrol. 43 (8), 1415–1434.

Peccerillo, A.,1998. Relationships between ultrapotassic and carbonate-rich volcanic rocks in Central Italy: petrogenetic and geodynamic implications. Lithos 43, 267–279.

Peccerillo, A., 2001. Geochemical similarities between the Vesuvio, Phlegrean Fields and Stromboli volcanoes: petrogenetic, geodynamic and volcanological implications. Mineral. Petrol. 73, 93–105.

Peccerillo, A., 2005. Plio–Quaternary Volcanism in Italy: Petrology, Geochemistry, Geodynamics. Springer-Verlag, Berlin. 365 pp.

Peccerillo, A., 2017. The Roman Province. In: Cenozoic Volcanism in the Tyrrhenian Sea Region. Advances in Volcanology. Springer, Cham. https://doi.org/10.1007/978-3-319-42491-0_4

Piana Agostinetti, N., Chiarabba, C., 2008. Seismic structure beneath Mt Vesuvius from receiver function analysis and local earthquakes tomography: evidences for location and geometry of the magma chamber. Geophys. J. Int. 175 (3), 1298–1308.

Pichavant, M., Scaillet, B., Pommier, A., Iacono-Marziano, G., Cioni, R., 2014. Nature and evolution of primitive Vesuvius magmas: an experimental study. J. Petrol. 55, 2281–2310.

Piochi, M., Ayuso, R.A., De Vivo, B., Somma, R., 2006. Crustal contamination and crystal entrapment during polybaric magma evolution at Mt. Somma-Vesuvius volcano, Italy: geochemical and Sr isotope evidence. Lithos 86, 303–329.

Plank, T., Langmuir, C.H., 1998. The chemical composition of subducting sediments and its consequence for the crust and mantle. Chem. Geol. 145, 325–394.

Rittmann, A., 1933. Die geologische bedingte evolution und differentiation des Somma-Vesuvius magmas. Zeitschrift für Vulkanologie 15, 1–2.

Rogers, N.W., Hawkesworth, C.J., Parker, R.J., Marsh, J.S., 1985. The geochemistry of potassic lavas from Vulsini, Central Italy, and implications for mantle enrichment processes beneath the Roman region. Contrib. Mineral. Petrol. 90, 244–257

Rosatelli, G., Castorina, F., Consalvo, A., Brozzetti, F., Ciavardelli, D., Perna, M.G., Bell, K., Bello, S., Stoppa, F., 2023. Elemental abundances and isotopic composition of Italian limestones: glimpses into the evolution of the Tethys. J. Asian Earth Sci. X, 9, 100136.

Rouchon, V., Gillot, P.Y., Quidelleur, X., Chiesa, S., Floris, B., 2008. Temporal evolution of the Roccamonfina volcanic complex (Pleistocene), Central Italy. J. Volcanol. Geotherm. Res. 177, 500–514.

Santacroce, R., 1987. Somma-Vesuvius. C.N.R. Quaderni de "La Ricerca Scientifica", 114, 251 pp.

Santacroce, R., Bertagnini, A., Civetta, L., Landi, P., Sbrana, A., 1993. Eruptive dynamics and petrogenetic processes in a very shallow magma reservoir: the 1906 eruption of Vesuvius. J. Petrol. 34, 383–425.

Savelli, C., 1967. The problem of rock assimilation by Somma-Vesuvius magma - I. Composition of Somma and Vesuvius lavas. Contrib. Mineral. Petrol. 16, 328–353.

Savelli, C., 1968. The problem of rock assimilation by Somma-Vesuvius magma - II. Composition of sedimentary rocks and carbonate ejecta from the Vesuvius area. Contrib. Mineral. Petrol. 18, 43–64.

Skora, S., Blundy, J.D., Brooker, R.A., Green, E.C.R., de Hoog, J.C.M., Connolly, J.A.D., 2015. Hydrous phase relations and trace element partitioning behaviour in calcareous sediments at subduction-zone conditions. J. Petrol. 56, 953–980.

Sparice, D., Scarpati, C., Mazzeo, F.C., Petrosino, P., Arienzo, I., Gisbert, G., Petrelli, M., 2017. New proximal tephras at Somma-Vesuvius: evidences of a pre-caldera, large (?) explosive eruption. J. Volcanol. Geotherm. Res. 335, 71–81.

Stoppa, F., Rukhlov, A.S., Bell, K., Schiazza, M., Vichi, G., 2014. Lamprophyres of Italy: Early Cretaceous alkaline lamprophyres of southern Tuscany, Italy. Lithos 188, 97–112.

Stormer, J.C., Nicholls, J., 1978. XLFrac: a program for interactive testing of magmatic differentiation models. Comput. Geosci. 4, 143–159.

Washington, H.S., 1906. The Roman Comagmatic Region. Carnegie Institution of Washington Yearbook, 36, 1–220.

Woelki, D., Haase, K.M., Schoenhofen, M.V. Beier, C., Regelous, M., Krumm, S.H., Günther, T., 2018. Evidence for melting of subducting carbonate-rich sediments in the western Aegean Arc. Chem. Geol. 483, 463–473.

Zhang, K.-J., Li, Q.-H., Yan, L.-L., Zeng, L., Lu, L., Zhang, Y.-X., Hui, J., Jin, X., Tang, X.-C., 2017. Geochemistry of limestones deposited in various plate tectonic settings. Earth-Sci. Rev. 167, 27–46.

Zollo, A., Gasparini, P., Virieux, J., Le Meur, H., De Natale, G., Biella, G., Boschi, E., Capuano, P.,

de Franco, R., dell'Aversana, P., de Matteis, R., Iannaccone, G., Mirabile, L., Vilardo, G., 1996. Seismic evidence for a low-velocity zone in the upper crust beneath Mount Vesuvius. Science 274(5287), 592–594.

Figure Captions

Figure 1. Distribution of potassic and ultrapotassic volcanism associated with calc-alkaline rocks in Italy (redrawn after Conticelli et al., 2007; Avanzinelli et al., 2008). Also shown are Cenozoic igneous rocks from peninsular Italy and Sicily with within-plate geochemical characteristics. The large arrow indicates the point of toroidal inflow through slab rifts.

Figure 2. Sketch map of the Somma-Vesuvius complex with red dots indicating the location of the samples studied. The dashed lines represent the boundaries of the craters of Somma (in blue), and Vesuvius (in magenta) as also reported in (a). (b) Location of Somma-Vesuvius. (c) Simplified geological map of Mt. Somma and Vesuvius, showing the outcrops of different eruptions.

Figure 3. (a) K_2O vs Na_2O diagram of Middlemost (1975) for the Somma samples and the lava of 1944 CE. (b) K_2O vs. SiO_2 diagram (Di Girolamo, 1984) for the Somma samples and the 1944 CE lava. The 1631-1944 volcanic products are shown. (c) TAS (Le Bas et al., 1986) and (d) R_1-R_2 (de la Roche et al., 1980) classification diagrams for the Somma samples and 1944 CE lava. The data used for comparison are from the following references: Avanzinelli et al., 2018; Ayuso et al., 1998; Belkin et al., 1993; Boari et al., 2009a, b; Cioni et al., 1998; D'Antonio et al., 1999; De Astis et al., 2006; Di Renzo et al., 2007; Fedele et al., 2008; Joron et al., 1987; Landi et al., 1999; Marianelli et al., 1999; Melluso et al., 2012, 2014, 2022; Piochi et al., 2006; Savelli, 1967, 1968.

Figure 4. Chondrite-normalized REE patterns for Mt. Somma lavas and dikes and 1944 CE lava compared with Mt. Vulture, Procida, Alban Hills, Roccamonfina, Ventotene, and Middle Latin Valley rocks (Beccaluva et al., 1991, 2002; Boari et al., 2009a, b; Conticelli et al., 2009b; De Astis et al., 2006). The normalization values are from Anders and Grevesse (1989).

Figure 5. (a-b) Nb/Yb vs. Th/Yb and Nb ppm vs. Nb/U; (c-d) La/Nb vs. Ba/Nb and La_N/Yb_N vs. Ba/Nb (e-f) Zr/Nb vs. Nb/U and Th/U diagrams for Mt. Somma lavas and dikes and lava of 1944 CE. The data used for comparison comes from the following references: Arevalo and McDonough (2010); Balassone et al. (2016); Belkin et al. (1993); Beccaluva et al. (1990,

1991, 2002); Boari et al. (2009a, b); Conticelli et al. (2009a, 2009b, 2015); D'Antonio et al. (1999); Mazzeo et al. (2014, 2018); Melluso et al. (2012, 2014, 2016); Plank and Langmuir (1998); Stoppa et al. (2014); Avanzinelli et al., (2018); Woelki et al. (2018); Klaver et al. (2015); Lustrino et al. (2012); Guarino et al. (2013); Fedele et al. (2008); De Astis et al. (2006).

Figure 6. Mantle-normalized multielement patterns for Monte Somma lavas and dikes and lava of 1944 CE compared with Mt. Vulture, Procida, Alban Hills, Roccamonfina, Ventotene, and Middle Latin Valley rocks (Beccaluva et al., 1991, 2002; Boari et al., 2009a, b; Conticelli et al., 2009b; De Astis et al., 2006). The normalization values are from Lyubetskaya and Korenaga (2007).

Figure 7. $^{87}Sr/^{86}Sr$ vs. $^{143}Nd/^{144}Nd$ and $^{87}Sr/^{86}Sr$ vs. SiO_2 and MgO diagrams for the Somma rocks. The data used for comparison are from the following references: D'Antonio and Di Girolamo (1994); D'Antonio et al. (1996, 1999, 2007); Mazzeo et al. (2014, 2018); Conticelli et al. (1997, 2002, 2007); Ayuso et al. (1998); De Astis et al. (2006); Pappalardo et al. (2002); Peccerillo (2005) and references therein; Boari et al. (2009a, b); Casalini et al. (2018); Rosatelli et al. (2023).

Supplementary Figure Captions:

Supplementary Figure 1. Details of the sampling of the caldera wall and outer slopes of Somma volcano.

Supplementary Figure 2. Variation diagrams of MgO (wt%) vs. major oxides (SiO_2, Al_2O_3, CaO, Fe_2O_{3t}, Na_2O, TiO_2, K_2O, P_2O_5, in wt%). The 1631-1944 CE volcanic products are from Belkin et al. (1993).

Supplementary Figure 3. Variation diagrams of MgO (wt%) vs. some trace elements (Sr, Ba, Rb, Zr, Nb, Y, Sc, V, F, Cl, and S in ppm). The 1631-1944 CE volcanic products are from Belkin et al. (1993).

Supplementary Figure 4. (a) The forsterite - $\delta^{18}O_{ol}$ covariation trend can be used to compare the unevolved lavas from Mt Somma and Mt Vesuvius magmatic activity with respect their degree of interaction with crustal CO_2 before/during differentiation. As the MgO decreases, the differentiation proceeds and the $\delta^{18}O$ values increase, indicating a higher degree of carbonate contamination. The stability of olivine likely indicates the presence of dolomitic carbonate in the assimilated material. (b, c) AFC model (DePaolo, 1981) assuming the most

primitive lava of this study and limestone and marl contaminants, as representative of the basement beneath Somma-Vesuvius.

Table captions

Table 1. New major (wt.%), trace elements (ppm) analyses and Sr isotopes of the Somma lavas and dikes.

Table 2. Oxygen isotopes on olivine and clinopyroxenes separated from the most representative Somma samples.

Supplementary Tables

Supplementary Tables 1 to 9. This file reports all the data produced in this study.

Figure 1

Click here to access/download;Figure;Figure 01 Somma.jpg

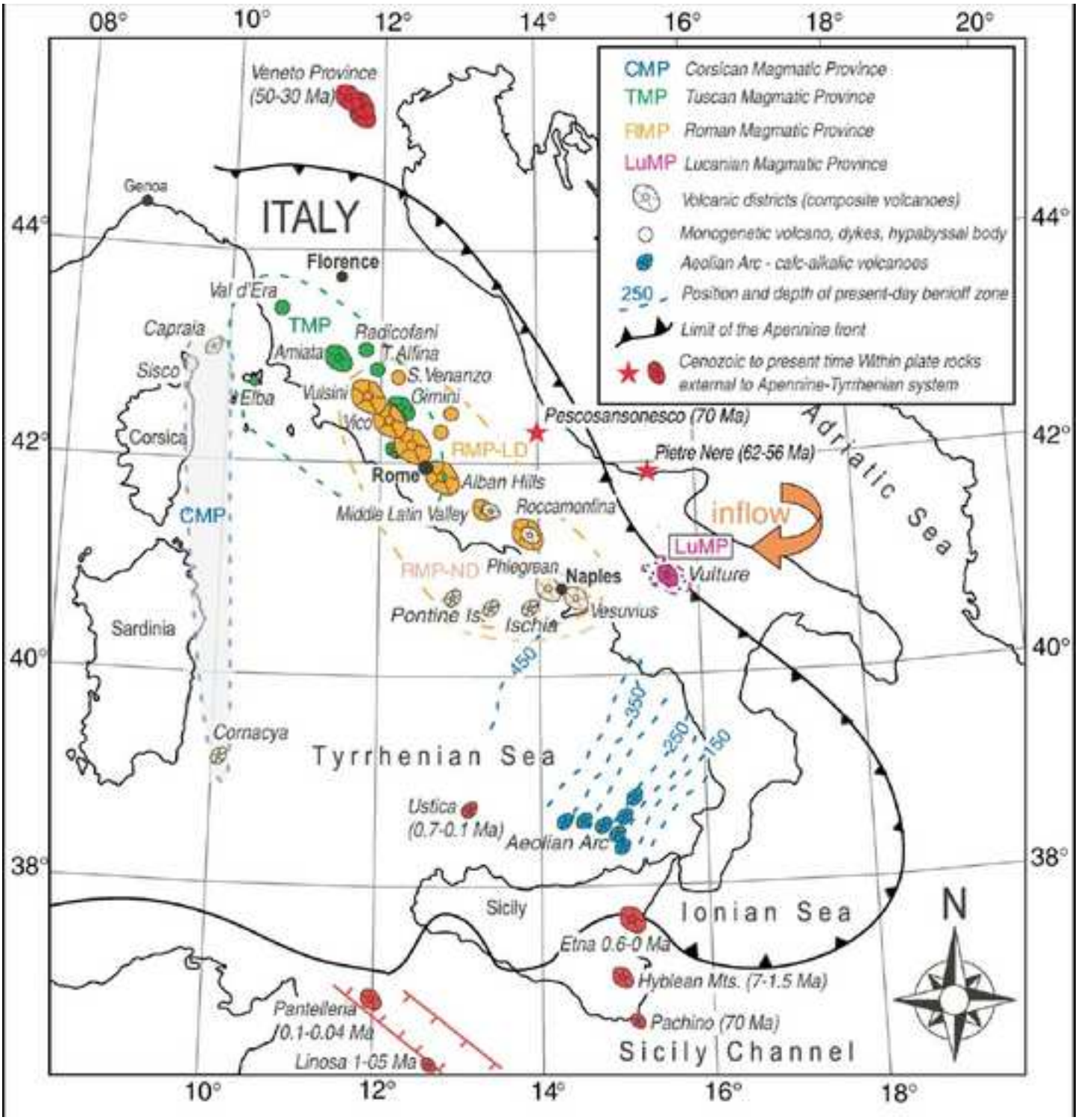

Figure 2

Click here to access/download;Figure;Figure 02.jpg

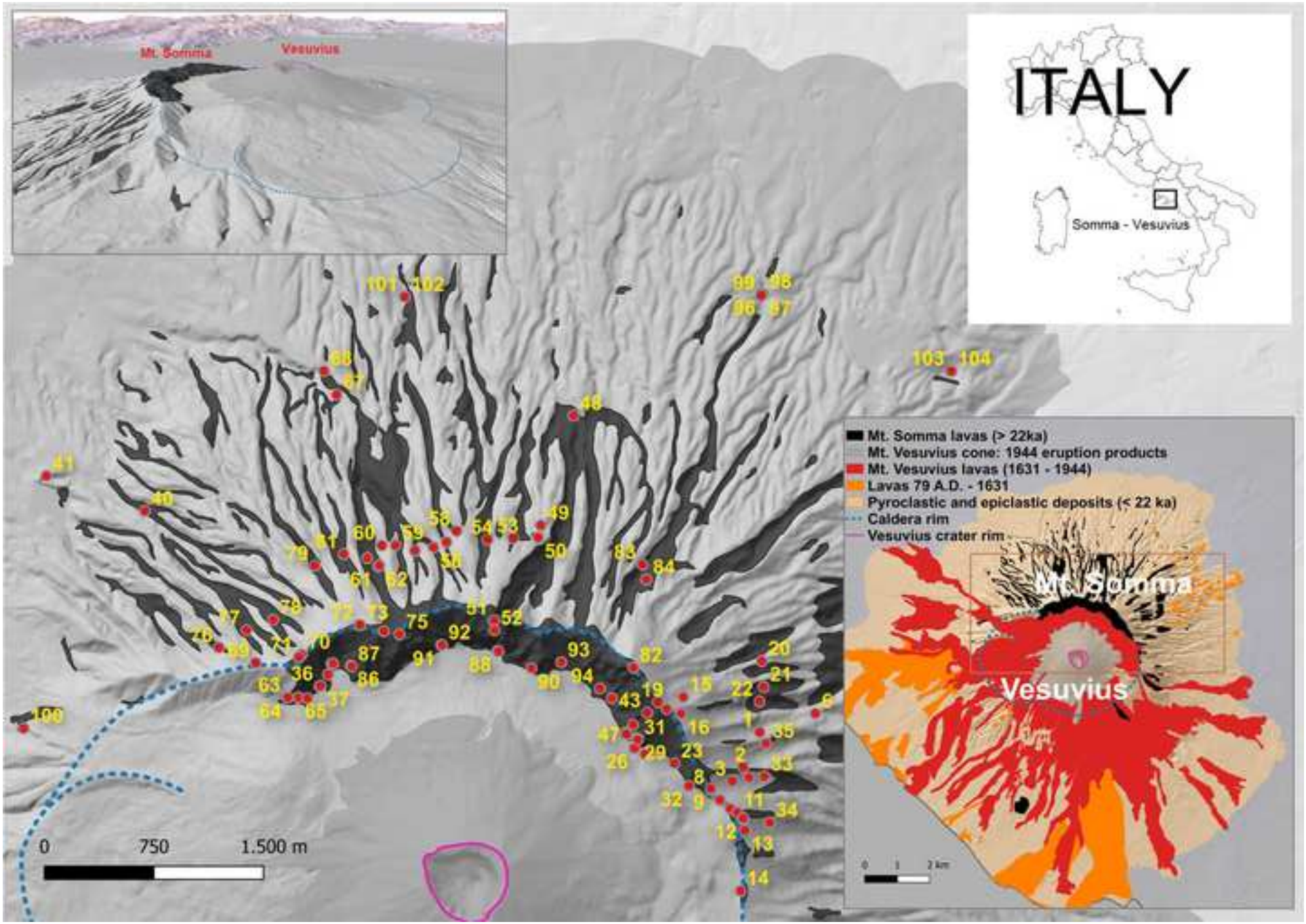

Figure 3

Click here to access/download;Figure;Figure 03 SV.jpg

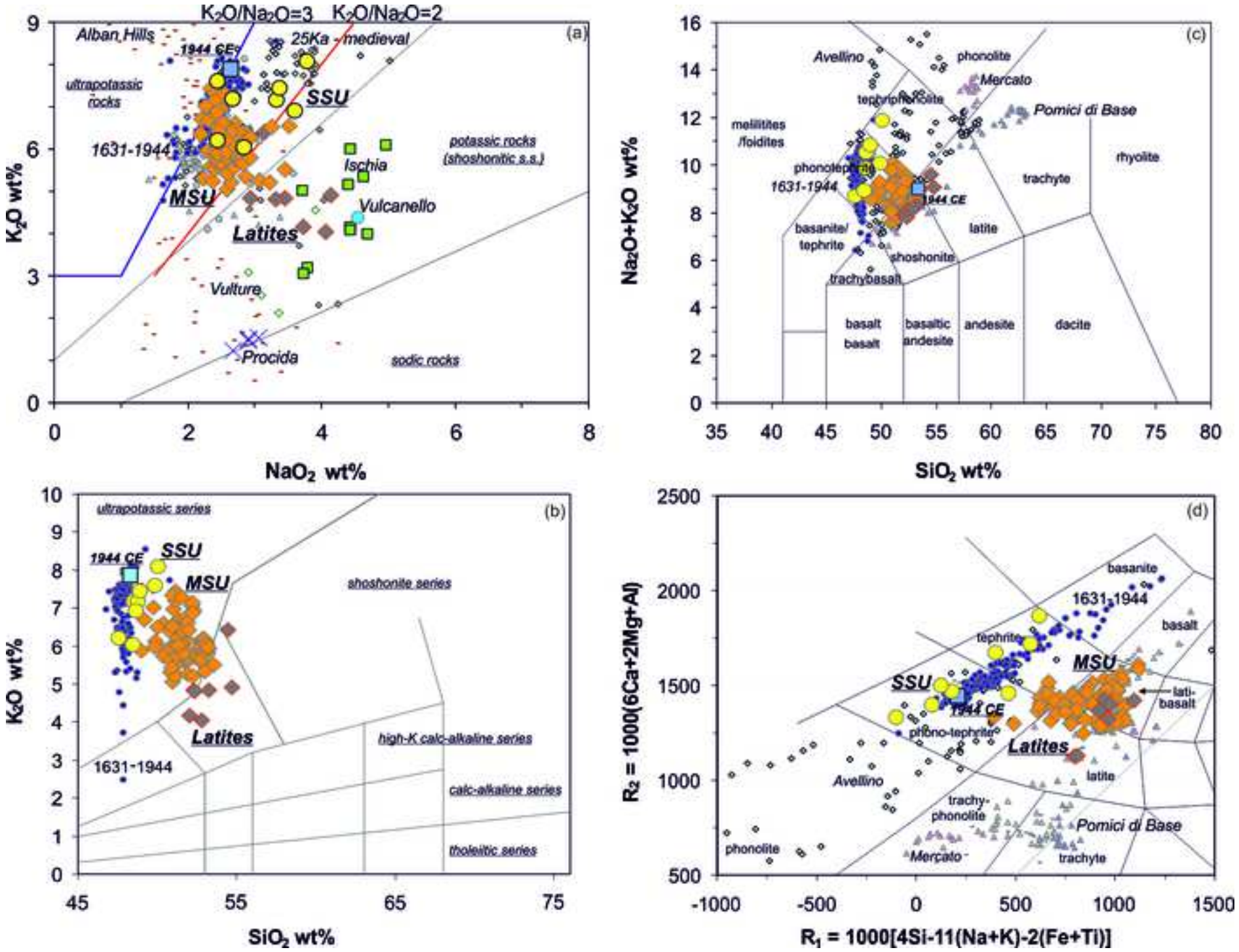

Figure 4

Click here to access/download;Figure;Figure 04 REE SV.jpg

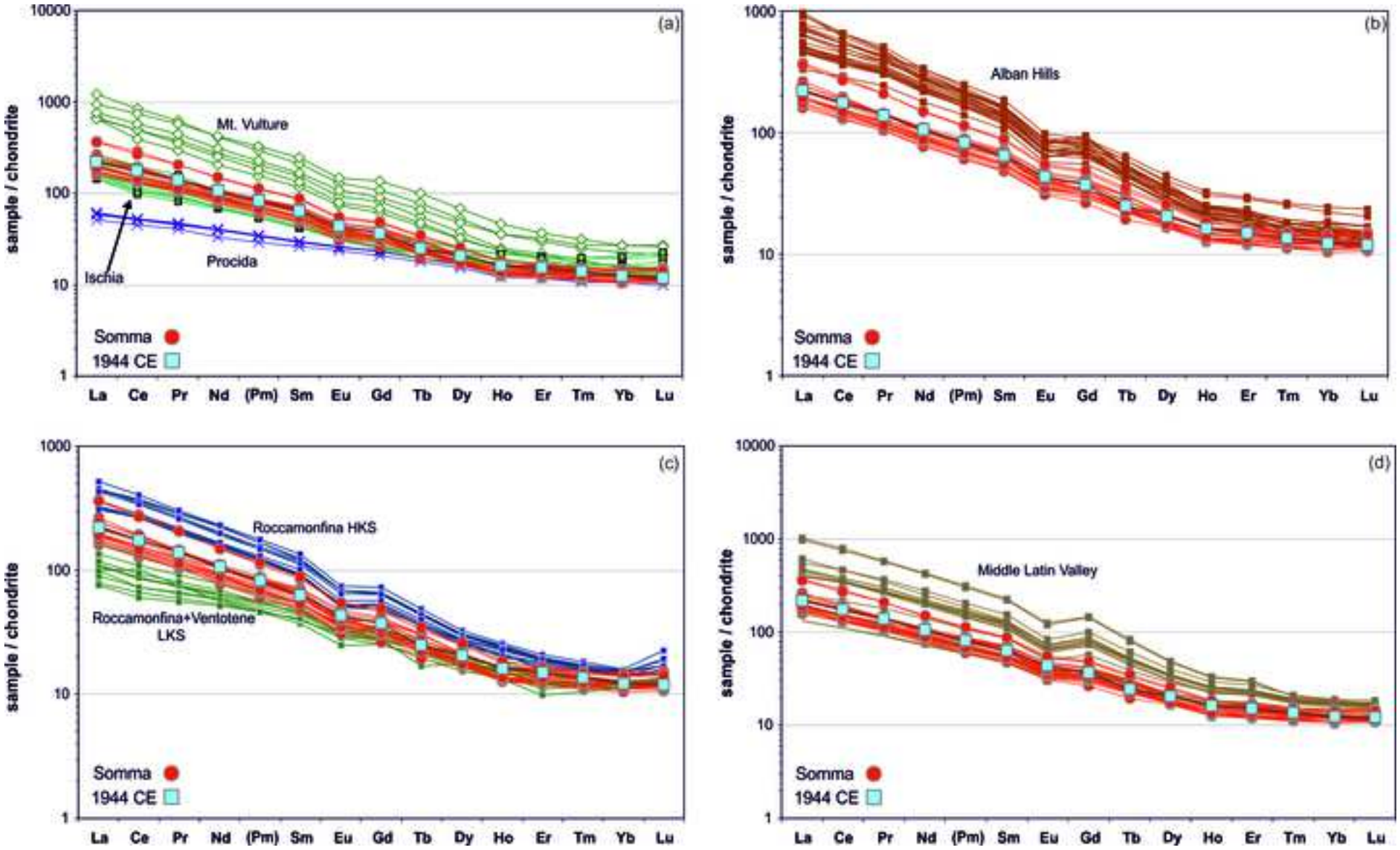

Figure 5

Click here to access/download;Figure;Figure 05 element ratio SV.jpg

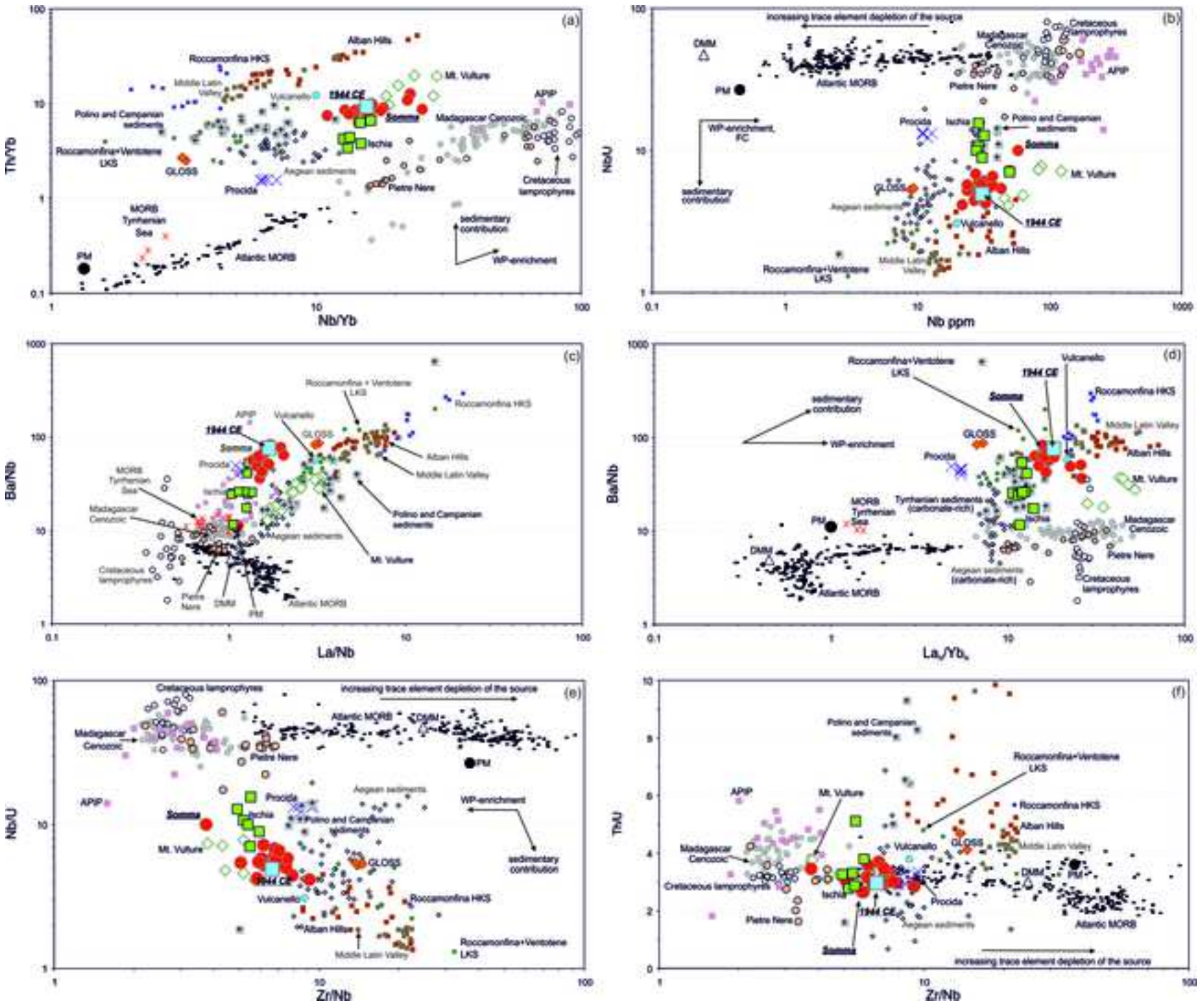

Figure 6

Click here to access/download;Figure;Figure 06 Wood SV.jpg

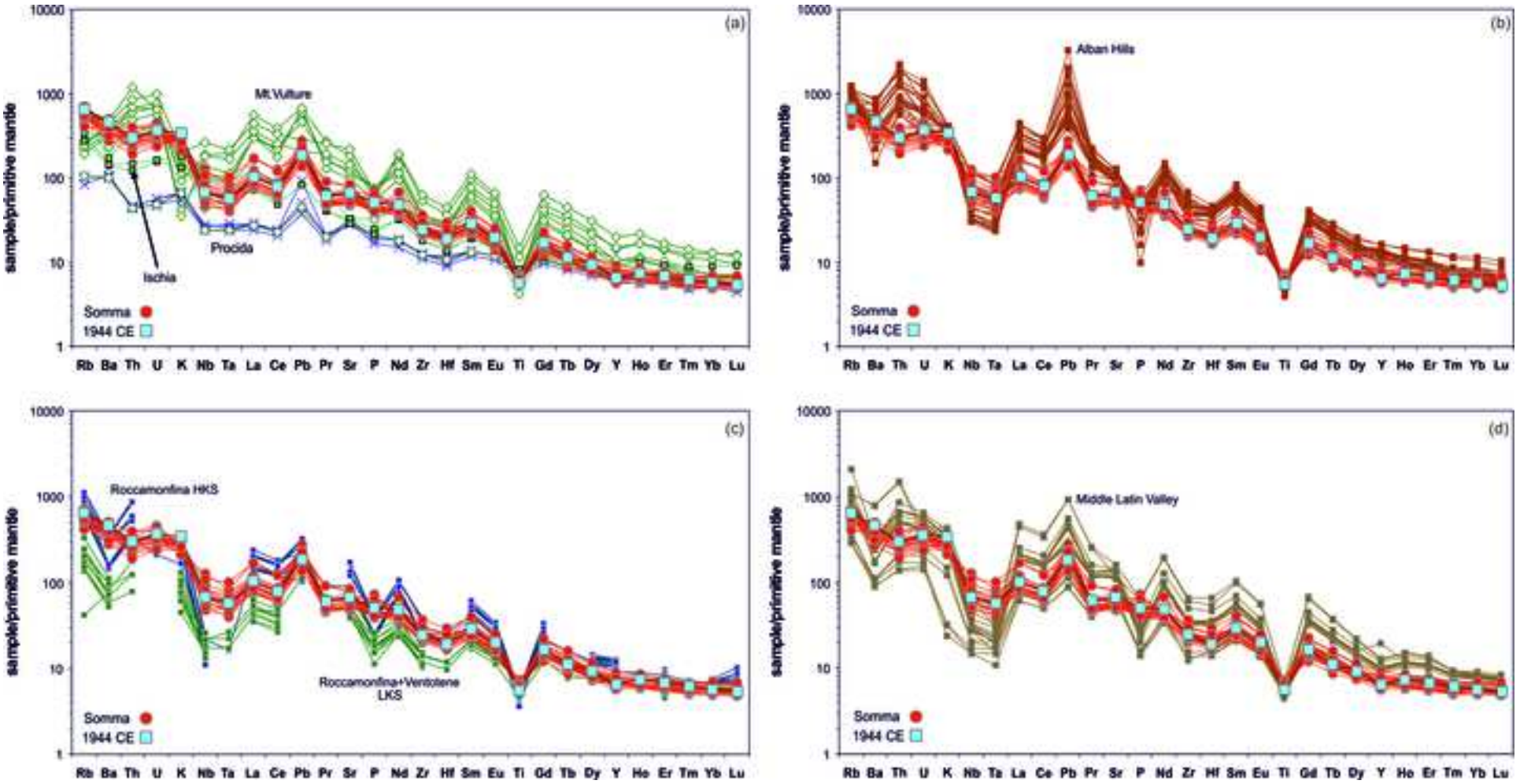

Figure 7

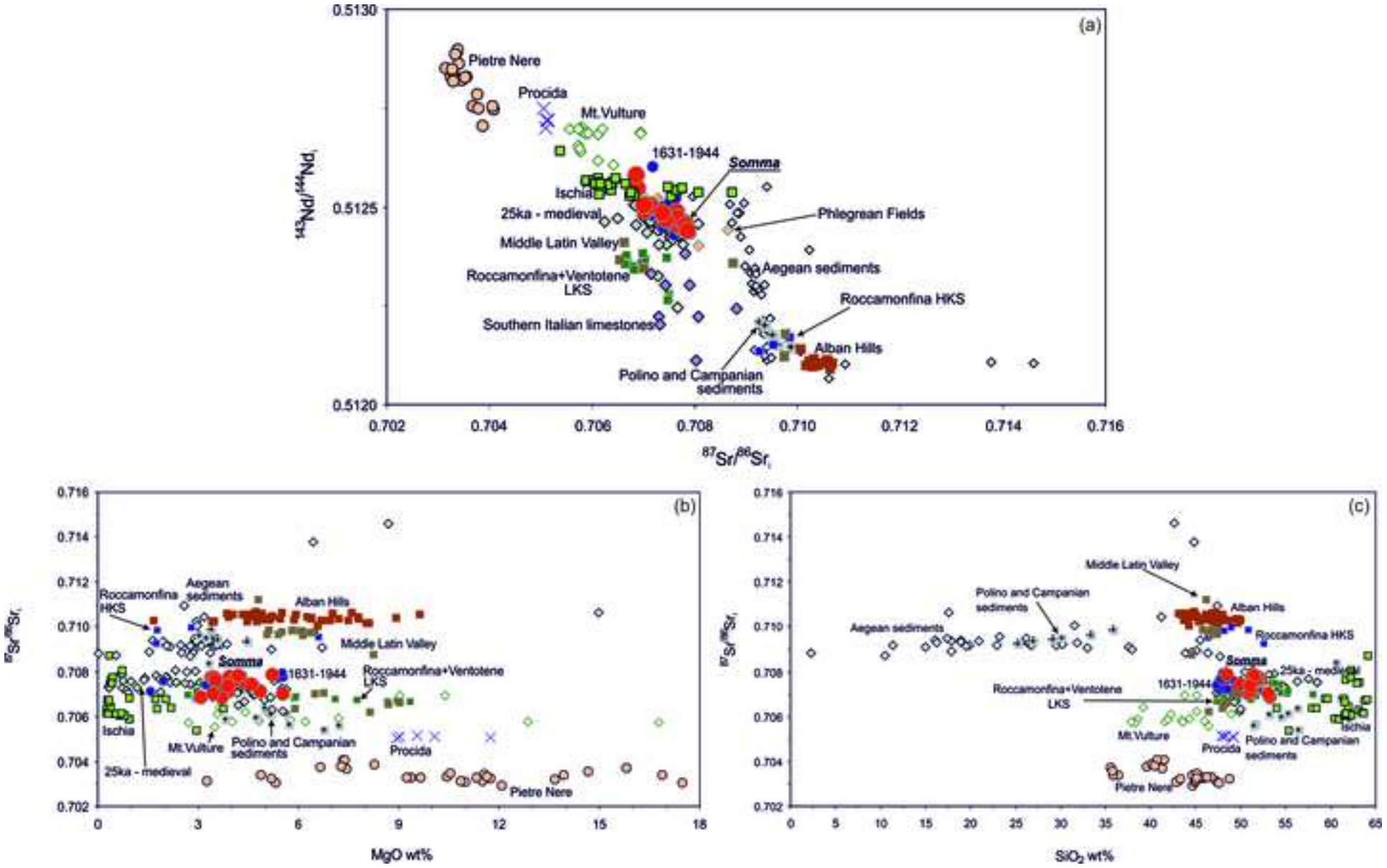

Table 1

Table 1. New major (wt.%) and trace elements (ppm) analyses and Sr isotopes of the Somma lavas and dikes.

	SSU group			MSU group														Latite group		
Sample	MRL3	MRL19	MRL97V	MRL59	MRL25	MRL41	MRL43	MRL74	MRL32	MRL6	MRL27	MRL50	MRL91	MRL24	MRL48	MRL35	MRL21	MRL37	MRL103	MRL104	V44lava
Type	lava	lava	lava	lava	dyke	lava	lava	lava	lava	lava	lava	lava	lava	dyke	lava	lava	lava	lava	lava	lava	lava
SiO_2 (wt%)	49.93	48.49	51.01	50.86	51.09	49.84	51.16	51.51	51.70	51.28	51.20	52.20	53.26	51.92	51.93	53.07	51.54	53.24	53.12	53.10	48.31
TiO_2	1.11	0.99	1.09	1.02	0.99	1.15	0.97	0.91	0.88	0.97	0.91	0.87	1.02	0.97	0.94	0.96	0.91	1.00	1.00	1.01	0.88
Al_2O_3	16.31	16.06	16.89	16.15	16.78	16.19	17.27	17.41	17.27	17.82	17.75	17.36	17.06	17.27	17.84	17.62	17.85	17.57	17.64	17.56	18.57
Fe_2O_3	8.61	8.45	7.91	8.52	8.11	8.80	8.25	7.95	8.08	7.53	7.27	7.26	7.99	8.34	7.32	7.93	7.13	7.73	7.82	7.85	8.26
MnO	0.15	0.15	0.14	0.14	0.14	0.15	0.14	0.14	0.13	0.13	0.12	0.12	0.13	0.14	0.12	0.13	0.12	0.13	0.13	0.13	0.15
MgO	4.58	5.21	3.88	5.53	4.86	4.38	4.32	4.19	4.10	3.94	3.91	3.86	3.71	3.52	3.47	3.45	3.40	3.07	3.28	3.13	3.55
CaO	9.01	10.63	7.56	9.43	9.22	9.09	8.82	8.27	8.19	8.61	8.12	7.98	7.52	7.50	8.15	7.25	8.13	7.42	7.51	7.32	8.46
Na_2O	2.66	2.76	3.49	2.09	2.24	2.82	2.49	2.46	2.78	2.68	2.49	2.30	3.47	2.33	2.49	2.71	2.51	2.81	2.56	2.78	2.65
K_2O	6.12	6.04	6.55	5.31	5.60	5.97	5.52	6.14	5.80	5.97	7.18	7.07	4.85	6.80	6.62	5.91	7.30	5.99	5.95	6.06	7.87
P_2O_5	1.01	0.81	0.97	0.60	0.61	1.09	0.62	0.59	0.62	0.68	0.66	0.61	0.63	0.81	0.71	0.61	0.70	0.64	0.61	0.67	0.76
LOI	0.14	0.71	0.39	0.03	0.24	0.06	0.06	0.32	0.08	0.24	0.13	0.08	0.06	0.01	0.36	1.09	0.15	0.42	0.51	0.65	0.39
sum	99.6	100.3	99.9	99.7	99.9	99.5	99.6	99.9	99.6	99.9	99.7	99.7	99.7	99.6	100.0	100.7	99.7	100.0	100.1	100.3	99.8
Sc (ppm)	21	24	14	27	24	22	20	21	18	19	18	21	18	17	17	17	14	16	18	17	13
V	212	219	250	202	254	183	201	185	155	188	191	202	238	219	195	206	177	228	148	157	212
Cr	100	bdl	bdl	74	bdl	60	109	56	62	60	90	6	50	90	10	40	bdl	53	bdl	bdl	30
Ni	46	32	20	37	30	30	47	36	40	30	47	16	40	50	18	30	28	35	bdl	bdl	20
Cu	59	95	120	70	120	80	68	61	58	80	52	45	50	80	59	60	56	93	30	40	110
Zn	69	88	80	75	70	60	69	78	78	70	83	83	80	80	88	80	88	84	90	90	80
Rb	214	302	321	271	322	325	188	242	267	264	247	256	230	280	254	294	244	241	255	242	298
Sr	750	993	1089	834	1006	753	806	938	849	1014	790	839	1225	957	892	1210	834	1305	958	984	1080
Y	25	27	23	21	23	19	21	22	23	20	24	23	27	22	23	22	24	30	26	26	22
Zr	201	215	192	180	201	170	178	195	222	191	188	219	217	207	220	217	230	309	255	260	205
Nb	22	27	33	25	33	24	24	29	32	31	28	29	58	35	29	43	30	50	37	37	31
Cs	12.4	17.7	19.0	13.1	15.0	19.6	10.0	12.3	13.6	14.5	9.9	12.5	12.8	14.1	12.3	15.8	12.5	13.4	13.4	13.3	17.6
Ba	1410	2120	2187	1622	2064	1783	1985	2281	1820	2370	1400	1869	2122	2139	2006	2109	1880	2559	1577	1587	2359
La	44.6	53.2	51.8	37.5	51.7	39.8	41.3	46.5	44.1	50.5	41.4	44.3	86.8	52.9	46.0	61.9	44.5	84.6	57.3	57.1	52.3
Ce	93.1	107.7	107.0	77.0	106.0	79.8	84.1	94.2	87.8	102.0	83.0	89.7	171.0	107.0	93.9	118.0	88.2	161.9	113	115	106
Pr	11.3	12.8	12.4	9.2	12.3	9.29	9.8	11.0	10.1	11.7	9.7	10.5	18.5	12.3	10.9	12.7	10.2	18.5	12.8	12.9	12.4
Nd	46.7	50.1	47.6	36.0	46.7	34.7	37.3	42.0	39.9	42.8	38.6	40.3	66.8	46.7	40.8	45.6	39.9	67.6	47	48.6	48.2
Sm	10.3	10.5	10.0	7.2	10.0	7	7.5	8.5	8.1	9.1	7.9	7.9	12.5	9.7	8.0	9.0	7.8	13.0	9	9.2	9.4
Eu	2.5	2.7	2.3	1.8	2.3	1.71	1.9	2.2	2.0	2.2	2.1	1.9	3.0	2.2	2.0	2.1	2.0	3.1	2.2	2.3	2.45
Gd	7.9	8.2	7.4	5.7	7.6	5.2	5.9	6.7	6.1	6.8	6.6	6.1	9.3	7.6	6.2	6.4	6.2	9.7	6.8	6.7	7.3
Tb	1.1	1.1	1.0	0.8	1.1	0.7	0.8	0.9	0.9	0.9	0.9	0.8	1.2	1.0	0.8	0.8	0.9	1.3	0.9	1	0.9
Dy	5.2	5.2	5.0	4.1	5.2	4	4.2	4.4	4.3	4.5	4.6	4.3	6.0	5.0	4.3	4.4	4.3	6.2	5.2	5.2	5
Ho	0.9	0.9	0.9	0.7	0.9	0.7	0.7	0.7	0.8	0.8	0.8	0.8	1.0	0.9	0.7	0.8	0.8	1.0	0.9	0.9	0.9
Er	2.3	2.5	2.4	1.9	2.5	1.9	1.9	2.0	2.0	2.2	2.2	2.1	2.7	2.3	2.0	2.3	2.1	2.6	2.6	2.6	2.4
Tm	0.3	0.3	0.3	0.3	0.3	0.27	0.3	0.3	0.3	0.3	0.3	0.3	0.4	0.3	0.3	0.3	0.3	0.4	0.35	0.37	0.33
Yb	2.0	2.1	2.1	1.8	2.0	1.7	1.8	1.8	1.8	1.9	1.9	2.0	2.3	2.0	1.9	1.9	1.9	2.3	2.4	2.4	2
Lu	0.3	0.3	0.3	0.3	0.3	0.26	0.3	0.3	0.3	0.3	0.3	0.3	0.4	0.3	0.3	0.3	0.3	0.3	0.37	0.36	0.29
Hf	4.9	4.6	4.5	4.1	5.0	3.7	4.0	4.3	4.6	4.3	4.2	4.9	5.1	4.6	4.8	4.3	4.8	6.6	5.6	5.7	4.3
Ta	1.3	1.4	1.8	1.6	1.8	1.2	1.5	1.7	1.7	1.7	1.4	1.8	2.5	1.9	1.9	2.3	1.6	3.1	2	2.2	1.7
Pb	bdl	36.3	30.0	23.5	31.0	30	27.6	33.7	23.6	29.0	19.6	29.7	26.0	30.0	29.1	40.0	29.2	33.4	33	31	27
Th	15.0	18.3	20.7	14.3	18.2	14.7	13.9	17.8	16.1	18.6	12.0	17.3	20.1	17.0	17.9	24.3	16.0	24.8	19.6	19.5	18.7
U	5.3	6.1	7.8	4.9	5.7	4.6	4.2	4.8	5.3	5.9	4.1	5.5	5.8	6.4	5.9	7.9	5.3	6.9	6.5	5.6	6.3
$^{87}Sr/^{86}Sr$	0.70743	0.70786	0.70737	0.70703	0.70713		0.70751	0.70782	0.70765	0.70781	0.70712	0.70769	0.70687	0.70763	0.70777	0.70701	0.70776	0.70688			
2s *10^6	±7	±8	±6	±6	±6		±7	±7	±7	±5	±7	±7	±6	±5	±7	±5	±6	±7			
$^{143}Nd/^{144}Nd$	0.51247	0.51244	0.51249	0.51249	0.51250		0.51248	0.51245	0.51247	0.51246	0.51250	0.51246	0.51258	0.51249	0.51244	0.51250	0.51245	0.51255			
2s *10^6	±4	±5	±6	±5	±6		±5	±4	±4	±5	±5	±5	±6	±4	±4	±5	±4	±5			

Note: bdl, below detection limits

Table 2. Oxygen isotopes on olivine and clinopyroxenes separated from the most representative Somma samples.

	sample	type	$\delta^{18}O/^{16}O_{cpx}$ (‰)	$\delta^{18}O/^{16}O_{ol}$ (‰)
SSU group	MRL19	lava	7.25	
	MRL82	lava	7.38	
MSU group	MRL59	lava	6.47	6.51
	MRL21	lava	6.81	7.20
	MRL100	lava	7.02	6.77
	MRL23	lava	6.76	6.56
	MRL24	dyke	6.31	6.83
	MRL27	lava	6.83	6.86
	MRL38	lava	6.55	6.39
	MRL37	lava	7.04	
	MRL7	lava	6.77	
	MRL93	dyke	6.81	
	MRL48	lava		6.99
Latite group	MRL51	lava	6.66	6.69
	MRL103	lava	7.90	

Suppl. Fig. 1

Suppl. Fig. 2

Suppl. Fig. 3

Suppl. Fig. 4

Click here to access/download

e-Component

Suppl. Figure 4.jpg

Suppl.Tables 1-9

Click here to access/download

e-Component

Suppl.Tables 1-9.xls

Supplementary Materials 2

Click here to access/download

e-Component

Supplementary Materials 2.docx

Highlights

Mt. Somma is significantly less silica undersaturated than the recent Vesuvius Cone

Geochemical and Sr-Nd-O data of the Somma rocks indicate subduction-related affinity

Subducted sedimentary rocks dominate the Somma trace element signature

Somma and Vesuvius lavas have an independent feeding system compared to RMP

Declaration of interests

☒ The authors declare that they have no known competing financial interests or personal relationships that could have appeared to influence the work reported in this paper.

☐The authors declare the following financial interests/personal relationships which may be considered as potential competing interests: